Performance Evaluation of a New Type of Titanium Nitride (TiN) Coated Twist Drill

by

Syed Mohtashim Nizam

A Thesis Presented to the

FACULTY OF THE COLLEGE OF GRADUATE STUDIES

KING FAHD UNIVERSITY OF PETROLEUM & MINERALS

DHAHRAN, SAUDI ARABIA

In Partial Fulfillment of the
Requirements for the Degree of

MASTER OF SCIENCE

In

MECHANICAL ENGINEERING

December, 1996

INFORMATION TO USERS

This manuscript has been reproduced from the microfilm master. UMI films the text directly from the original or copy submitted. Thus, some thesis and dissertation copies are in typewriter face, while others may be from any type of computer printer.

The quality of this reproduction is dependent upon the quality of the copy submitted. Broken or indistinct print, colored or poor quality illustrations and photographs, print bleedthrough, substandard margins, and improper alignment can adversely affect reproduction.

In the unlikely event that the author did not send UMI a complete manuscript and there are missing pages, these will be noted. Also, if unauthorized copyright material had to be removed, a note will indicate the deletion.

Oversize materials (e.g., maps, drawings, charts) are reproduced by sectioning the original, beginning at the upper left-hand corner and continuing from left to right in equal sections with small overlaps. Each original is also photographed in one exposure and is included in reduced form at the back of the book.

Photographs included in the original manuscript have been reproduced xerographically in this copy. Higher quality 6" x 9" black and white photographic prints are available for any photographs or illustrations appearing in this copy for an additional charge. Contact UMI directly to order.

UMI

A Bell & Howell Information Company
300 North Zeeb Road, Ann Arbor MI 48106-1346 USA
313/761-4700 800/521-0600

PERFORMANCE EVALUATION OF A NEW TYPE OF TITANIUM NITRIDE(TiN) COATED TWIST DRILL

BY

SYED MOHTASHIM NIZAM

A Thesis Presented to the
FACULTY OF THE COLLEGE OF GRADUATE STUDIES
KING FAHD UNIVERSITY OF PETROLEUM & MINERALS
DHAHRAN, SAUDI ARABIA

In Partial Fulfillment of the
Requirements for the Degree of

MASTER OF SCIENCE
In

MECHANICAL ENGINEERING

DECEMBER 1996

UMI Number: 1385297

UMI
300 North Zeeb Road
Ann Arbor, MI 48103

KING FAHD UNIVERSITY OF PETROLEUM AND MINERALS
DHAHRAN, SAUDI ARABIA
COLLEGE OF GRADUATE STUDIES

This thesis, written by

Syed Mohtashim Nizam

under the direction of his Thesis Advisor, and approved by his Thesis committee, has been presented to and accepted by the Dean, College of Graduate Studies, in partial fulfilment of the requirements for the degree of

MASTER OF SCIENCE IN MECHANICAL ENGINEERING

Thesis Committee :

Dr. A.N. Shuaib (Chairman)

Dr. B. S. Yilbas (Member)

Joachim Nickel

Dr. J. Nickel (Member)

Dr. S.O. Duffuaa (Member)

Department Chairman

Dean, College of Graduate Studies

Date: 26-4-97

This thesis is dedicated to my parents, brothers and sisters, for the happiness they have given me, and the joys we have shared.

ACKNOWLEDGEMENT

First and foremost all praise be to Allah(subhanahu-wa-taala) who gave me the opportunity to carry out this work. I can never thank him enough for all that he has given me. I seek his forgiveness, mercy and guidance.

Acknowledgement is due to **King Fahd University of Petroleum and Minerals** for providing the material and financial support for this research work. I am thankful to the Chairman M.E. department, **Dr. Mohammed O. Budair** for his cooperation and support. I am also thankful to the Manager, Energy Research Laboratory(ERL) for allowing me to use the Tendatron Accelerator facility. Thanks are also due to the people at the M.E. workshop for their assistance and cooperation, during the drilling experiments.

I am grateful to my thesis committee chairman **Dr. Abdel Rahman N. Shuaib**, for his help and advice. I have learnt a lot from him for which I am thankful. Working with him was an unforgettable experience.

I am also thankful to **Dr. Bekir S.Yilbas**, who provided the new coated drill bits for these experiments and also accepted to be a member in my thesis committee. Thanks are due to Dr. **Joachim Nickel** for his insightful comments and practical help. I am also thankful to **Dr. Salih O. Duffua** for his expert comments on the part relating to design of experiments and statistical analysis.

Contents

List of Figures

List of Tables

THESIS ABSTRACT

Name: SYED MOHTASHIM NIZAM

Title: PERFORMANCE EVALUATION OF A NEW TYPE OF TITANIUM NITRIDE (TiN) COATED TWIST DRILL

Major Field: MECHANICAL ENGINEERING

Specific Area: MANUFACTURING & MATERIALS

Date of Degree: December 30th 1996

Titanium Nitride (TiN) coated tool materials have become increasingly popular in the metal cutting industry because of their improved resistance to wear and friction. In this study the machining performance of a new type of Titanium Nitride(TiN) coated twist drill with an intermediate plasma nitrided layer was evaluated and compared to the performance of commercial TiN coated twist drills.

The performance variables used include the drilling thrust force, torque, drill wear and hole surface roughness data, obtained from drilling experiments conducted on AISI 303 stainless steel workpiece material. The matched pair statistical testing method was introduced to quantitatively compare the relative performance of the two types of drills. Wear patterns on the flank face and the chisel edges obtained by using micro-PIXE (Particle Induced X-Ray Emission) technique were also analyzed.

The experimentally coated drills showed better performance, as was observed from its relatively lower median values of torque, flank wear, and hole surface roughness compared to the commercial drills. The median values of the thrust force were found to be approximately equal for both types of drills. The PIXE results indicate that wear on the flank face of the new drill takes place by abrasion and wear on the flank face of the commercial drill takes place mainly by cracking and spalling of the TiN coat.

Master of Science Degree

King Fahd University of Petroleum and Minerals, Dhahran.

ملخص البحث

الاسم: سيد محتشم نظام

عنوان البحث: تقويم أداء مثقاب فولاذي حلزوني جديد مطلي بنتريد التيتانيوم

التخصص الرئيس: الهندسة الميكانيكية

مجال البحث: هندسة التصنيع و علوم المواد

تعود الزيادة المطردة في استخدام عددُ قطع المعادن المطلية بنتريد التيتانيوم في الصناعة إلى حسن مقاومتها للتآكل و تقليلها للاحتكاك. و في هذه الدراسة يتم تقويم أداء مثقاب فولاذي حلزوني جديد مطلي بنتريد التيتانيوم فوق طبقة منتردة بالبلازما و مقارنته بأداء مثقاب فولاذي حلزوني تجارى مطلي بنتريد التيتانيوم.

و تشمل عناصر المقارنة بيانات القوة و العزم و التآكل و درجة خشونة سطوح الثقوب الناتجة عن حفر فولاذ مقاوم للصدأ. و تم تطبيق طريقة الاختبار الإحصائي للازواج المتزائمة للمقارنة الكمية للأداء النسبي للنوعين. كما تم تحليل أنماط تآكل السطح و طرف الأزميل باستخدام الأشعة السينية الجزئية المنبعثة بفعل الجسيمات المستحثة (micro-PIXE).

و قد أظهرت النوعية الجديدة من الثقابات المطلية أداء نسبيا افضل من الثقابات التجارية خلال قيم العزم و تآكل السطح و خشونة سطح الثقوب. و وجد أن قيم قوة القطع متساوية تقريبا لكلا المثقابين. و بينت نتائج الأشعة السينية الجزئية المنبعثة (micro-PIXE) أن تآكل سطح المثقاب الجديد ناتج عن عملية الاحتكاك و أن تآكل سطح المثقاب التجاري ناتج عن تشقق و تصدع طبقة طلاء نتريد التيتانيوم.

درجة الماجستير فى العلوم

جامعة الملك فهد للبترول و المعادن – الظهران

Chapter 1

INTRODUCTION

Drilling is one of the most important operations performed in the machining industry. From automobile parts to aircraft components, almost every manufactured product requires holes to be drilled for the purpose of assembly or creation of fluid passages, etc. According to a study by Billau and Heginbotham[1], hole making operations like drilling, boring and tapping, constitute about one third of all machining operations. Drilling is usually the most efficient and economical method of cutting a hole in solid metal when the hole size ranges from one eighth to one and a half inch(3.2mm to 38.1mm) in diameter. The metal cutting drill bit is a rotary end-cutting tool with one or more cutting lips and usually two or more cutting edges. Figure 1.1 shows the cutting edges of a two flute twist drill. The two main cutting edges are designed to produce identical chips and the central web region or the chisel edge extrudes metal at the center of the hole. The two flutes transport the chips out of the drilled hole.

The material of the cutting tool has a profound effect on the tool life, rate of metal removal, the surface finish produced, ability to give the required tolerance,

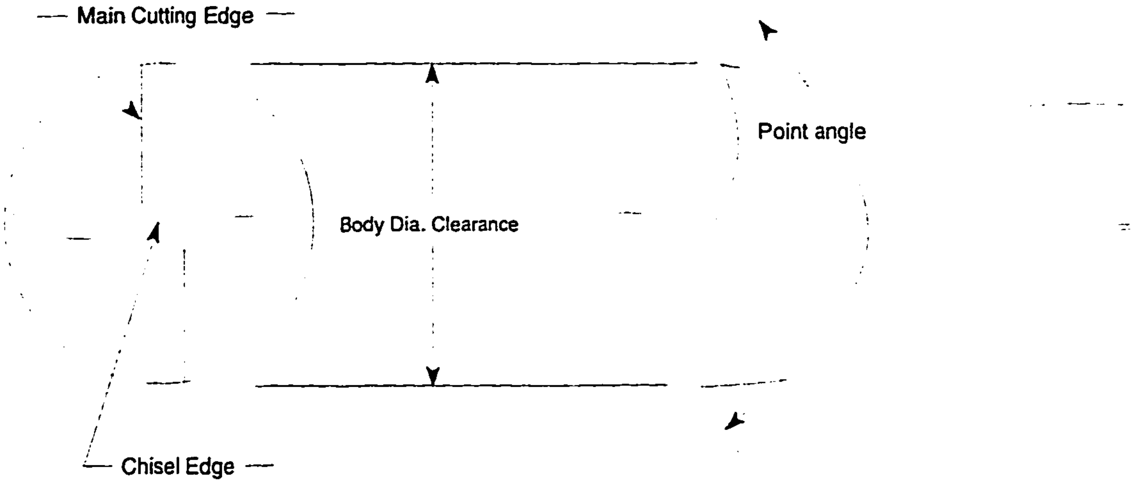

Figure 1.1: Cutting Edges of a Two Flute Twist Drill

and the overall economy of the process.

Most of the drills used in industry are made of common grade high speed steel(HSS) such as the AISI[1] designated M_7-molybdenum type, which provides, at a comparatively low cost, toughness, strength and high temperature hardness suitable for most drilling applications. However, titanium nitride(TiN) coated high speed steel drills are fast replacing uncoated high speed steel tools and uncoated carbide tools as they provide improved tool life at higher material removal rates and better drilled hole surface finish. To improve the performance of the drill bits through the use of hard coatings such as TiN, TiC, etc., the fundamental requirement is the adhesion of the coating to the substrate. Therefore the possibility of further improvements in the performance of such coatings, by modifications of the coating process itself, which may improve adhesion of the coating to the substrate

---

[1] AISI=American Iron and Steel Institute

is of major interest to researchers.

In line with this development a new physical vapor deposition(PVD) coating technique was reported by Yilbas et al [2], in which a thin nitride diffusion layer is applied to the substrate prior to the application of TiN coat. This is expected to provide better coating adhesion to the substrate, increase the tool life and enhance overall tool performance. Consequently, investigation into the basic cutting performance data of these tools needs to be established and reported in order to benchmark these tools with commercially available TiN coated cutting tools.

The objective of the present study is to investigate the drilling performance of HSS twist drills which were TiN coated by the PVD coating technique reported in [2]. The overall machining performance of the drill bits will be evaluated by conducting drilling experiments on stainless steel work pieces under actual cutting conditions. The performance of these drills will be compared to that of a commercially available TiN coated drill bits. The machining performance of the drills will be evaluated in terms of drilling thrust force, drilling torque, quality of the drilled holes in terms of surface finish, and the wear on the drill flank face. In addition to the conventional optical wear measurements, the micro-PIXE (Proton Induced X-Ray Emission) technique, which was used before by Shuaib, Nickel and Ahmed [3] in the wear investigations of uncoated tungsten carbide(WC) cutting tools, will be applied to determine the wear behavior of the drill bits.

The thesis organization is as follows: Chapter-2 provides a review of the literature and Chapter-3 covers the experimental design, experimental setup and the procedure used to conduct drilling experiments for obtaining machining data required for the evaluation of the performance of the twist drills. The results and discussions of the machining tests are presented in Chapter-4. In Chapter-5 the relative performance of the two types of TiN coated twist drills is evaluated by using appropriate statistical analysis techniques. The conclusions and recommendations are given in Chapter-6.

Chapter 2

LITERATURE REVIEW

An extensive literature review shows that the development of tool materials had taken place gradually and was closely related to the demand for materials which could tolerate the severe chemical, physical and mechanical wear processes. The commonly used tool materials include high speed steels(HSS). cemented carbides, coated tools, ceramics and polycrystalline diamonds. Tool materials in machining must meet the following requirements: High hardness and wear resistance, high toughness, high hot hardness, deformation resistance, good chemical stability, chemical inertness with work material, stiffness, ease of fabrication, availability and low cost. High speed steels find their application in drills, reamers, milling cutters because they provide the toughness required by the impact of multi-tooth cutters.

Research on tool material development has attempted to increase the hardness of the tool surface so as to machine difficult -to-machine or conventional materials at higher cutting speeds thereby increasing the production rate. Consequently new tool materials having high hardness such as carbides, ceramics and cermet tools were developed. Unfortunately, these tools were extremely brittle and could not give satisfactory performance in applications requiring shock resistance. This led to the most important development in the cutting tool industry viz: the introduction of composite tools or coated tools. These tools essentially consist of a core material which is mostly made up of high speed steel or cemented carbide, coated with a thin layer of ceramic material such as TiC, TiN, or Al_2O_3 [4]. The technological and economical performance of cutting tools have been a major subject of study for the past several decades. With the increasing number of new tool materials, it becomes necessary to benchmark these tools with the one's being used in industry. This will not only help in evaluating the effectiveness of the new tools, but will also provide the information necessary for the development of even better tool materials.

Although research in the field of metal drilling started in the beginning of the 19th century [5], extensive work is still being done in this field to better understand the basic factors which affect the useful life of a drill bit [6]. Initial research in the area of drilling was focussed on finding the thrust force and torque required in drilling various materials. Shaw [7] for the first time in 1957 used dimensional analysis to develop equations for the torque and the thrust force in drilling SAE[1]3245 nickel chromium steel. Using regression analysis approach it was shown that the torque and thrust is a function of the feed, diameter of the drill, the Brinell hardness number of the work material, and the ratio of the length of the chisel edge to the drill diameter. It was argued that the effect of cutting speed is not significant on the thrust and torque. The equations for the torque and thrust force derived in this study is valid for drilling materials having Brinell hardness less than 250HB. The thrust and torque equations show that changes in the drill diameter has a large

---

[1] Society of Automotive Engineers

effect on torque compared to changes in feed, whereas the effects of feed and drill diameter on the thrust force are nearly equal.

Pai, Bhattacharyya and Sen [5] in 1965, investigated the torque developed in drilling ductile materials, and determined theoretical values for the torque by proceeding from the initial properties of the work material and the cutting conditions. All the experiments in this study were conducted with pilot holes to avoid the extrusion process at the chisel edge. This limits the effectiveness of the torque equation as the drilling process involves the action of both the cutting lip as well as the chisel edge. This is due to the fact that extrusion as well as cutting action takes place at the chisel edge [7]. In 1968 Billau and Heginbotham [1] studied the general factors which could affect the performance of twist drills. The effect of three factors; speed, feed and the drill length projection from the chuck were investigated using a three factor two level experimental design matrix with a single replication. It was shown that the drill projection is quite significant in establishing the drill failure. The wear criterion used in this study was the decrease in thickness of the lip at the outer corner of the lip. The work of Ham and Ermer [8] in 1968 is of value in comparing the performance of different tools. In their study the cutting performance in terms of tool life of titanium carbide tool was compared with that of a cast-iron grade tungsten carbide tool. They developed tool life relationships from a limited number of tests using experimental design technique.

It has been observed that the drill life shows large variation in actual industrial conditions. This fact becomes important in planned tool replacement situations in automated machining operations where the tools are replaced at predetermined intervals. This scatter in tool life was shown to be strongly related to the variations in the hardness of the work material [9], which also influences the torque and thrust force in drilling operations [7], hence careful analysis is necessary before using torque and thrust models for predicting drill failure. Some researchers have taken this fact into consideration while developing torque and thrust equations. Worth mentioning among them are the models developed by Subramanian and Cook [9], which can be used when the hardness variation within the work piece material is of the order of 5 percent. Lenz, Mayer and Lee [10] conducted studies using High Speed Steel drills with the purpose of establishing a suitable drill life criterion. They found that the wear on the outer margin of the drill could be taken as one such criterion. Osman, Xistris and Chahil [11] studied the dynamic fluctuations of torque and thrust in drilling mild steel and found that these fluctuations are stationary random and gaussian processes. They concluded that the total thrust and torque are composed of two components: a mean static component which is usually overlapping with another dynamic fluctuating component. For their particular cutting conditions using mild steel they found that the value of the dynamic component of the thrust to be about 21 percent of the mean static thrust. Similarly the value of the dynamic component of the torque was found to be about 28 percent of the mean static torque.

Thangaraj and Wright [12] used the gradient of thrust force as a monitor of drill wear. They showed that this parameter can be used to develop a feedback control system which can be used to predict incipient drill failure. It was found that the gradient of thrust force is a better indicator of failure than the gradient of torque because of the high noise levels associated with the torque signals.

Drill life can be affected by several variables such as drill diameter, web thickness, helix angle, point angle, workpiece material and process variables like speed and feed rate. A review of the literature shows that no researcher has considered all these variables simultaneously in developing predictive models for the tool life, thrust or torque. As an example Jalali and Kolarik [13] have used the speed, feed and the drill diameter and the workpiece hardness as the variables in developing tool life, thrust and torque models. Rubenstein [14] in 1991 studied the torque and thrust force in twist drilling and developed empirical models for their prediction. Agapiou [15] in 1993 studied the performance of a four fluted twist drill and compared it with that of a two fluted drill. A significant observation from using such four fluted drills was the better hole quality obtained and the reduction in vibrations. However, increasing the number of flutes decreased the drill strength. The thrust force and torque were also measured and modelled as a function of speed, feed, diameter and hardness of the material and tool geometry. The effect of speed was found to be negligible in this case. Lin and Ting [16] studied the effect of flank wear on the average cutting force and presented a relationship between the cutting force, tool wear and other cutting parameters. The effect of feed rate, depth of cut and tool wear on the cutting force was found to be significant while the effect of cutting speed was found to be negligible.

While most of the earlier studies report the effect of cutting speed on forces and torque as being negligible for a wide range of cutting conditions, drill sizes, and variety of materials, recent research in this area shows that the speed may have a significant effect on the cutting forces and torque. For example the work done by Watson [17] showed that increasing the cutting speed would lead to greater force initially and then decreasing force as the speed was further increased, similar results were also found for the torque. The author has given interesting explanations for this trend and attributed it to the phenomenon of blue brittleness or dynamic strain ageing. Rubenstein [14] has given a different explanation for this trend using theoretical expressions for the thrust and torque. Sadat [18] also found that increasing the cutting speed decreases the cutting force and torque in machining Inconel-718 superalloy. The presence of built-up-edge and seizure is given as the reason for this observation.

The benefits of TiN and TiC coatings became apparent in the late 1960s when it was found by some watch manufacturers in Switzerland that such coatings improve the wear resistance of watch components [19]. The first commercially available coated carbide tools were made by *Sandvik*^{R} and were of the chemical vapour deposition (CVD) type [19]. The coating was deposited on the tools by passing titanium tetrachloride vapour, hydrogen and methane over the carbide tools which were heated to a temperature of around 1200^{0}C. The reaction between $TiCl_4$ and CH_4 resulted in the formation of TiC and HCl. The TiC was deposited in a very fine form on the carbide substrate. Although the TiC coated carbide tools functioned better than the uncoated tools, this process was not applicable to all types of tool materials because most of the commonly used tool materials such as high speed steel(HSS) soften at a temperature well below 1200^{0}C. It was also found that TiN coated tools has a greater wear resistance compared to TiC coated tools. Subrmanian et al[20] conducted machining experiments on TiN coated HSS turning tools. The base material of the tool was AISI T_1 and AISI T_{15} high speed steel and the work piece material used was AISI 4340 steel. The coating was deposited by radio frequency (rf) sputtering technique and the coating thickness was varied from 4μm to 5 μm. Using tool failure as tool life criterion they found that 2-4 times increase in tool life occurred as compared to uncoated tools.

Henderer [21] studied the effect of TiN coating on M_7 HSS drill bits. The drill size used in their experiments was 6.35 mm diameter and the work piece material used was AISI 4134. The thickness of the coating was 1.5 μm. The tool life criterion used in this study was the time required to extend the wear land to the full width of the cutting edge. An interesting finding made by Henderer [21] was the fact that tool life of coated tools was less sensitive to feed and speed than that of uncoated drills. He also found that the torque and the thrust for the coated drills was about 35 to 43 percent less than those of uncoated drills for the same drilling conditions. He concluded that this significant reduction in the cutting forces may be due to the reduced friction when the TiN coated drills are used. Dearnley and Trent [22] conducted many experiments on CVD coated cemented carbide tools. They investigated three different coatings viz: TiC, TiN and Al_2O_3, in order to study the type of wear mechanisms which are responsible for the deterioration of the coatings. They found that on the rake face of TiC coated tools the primary wear mechanism is atomic diffusion and discrete plastic deformation, while for TiN and uncoated cemented carbide tools, the crater face wear mechanism was mainly atomic diffusion. In case of Al_2O_3 coatings the principal wear mechanism was found to be plastic deformation.

Konig, Kauven and Droese [23] investigated the effect of coating thickness on the performance of gear hobbing tools and drill bits. The drilling conditions were experimentally simulated by rubbing the drill against two friction blocks. Various coating thicknessess were studied to find the best thickness for tool life enhancement. They found that a thickness of 4 μm gave the longest tool life. The tool life criterion used in this study was flank wearland width VB = 0.2 mm. The author in his research has emphasized the need for developing a simple experimental procedure for tool wear and tool life investigations.

Randhawa [24] investigated some of the characteristics of PVD TiN coated drill bits, end mills and threading tools. He addressed the important issue of the effect of surface finish, surface topography, coating thickness and metallurgical characteristics of the coatings on tool performance. His results suggest that the tool life is a strong function of coating thickness. Munz [25] studied the oxidation behavior of TiN and TiAlN coated drill bits in order to find the oxidation resistance of such films in machining environment. He found that TiN coated tools showed low oxidation resistance and tended to oxidize at about 550 ^{0}C. Konig, Fritsch and Kammermeier [26]showed that the life of coated tools is influenced by the thermal conductivities of the coating material. In their investigations with TiAlN, TiN and TiC coated HSS M_{47} inserts, they found that TiAlN which has a higher thermal conductivity compared to TiC and TiN gave relatively higher tool life. They also showed that hard surfaces act as solid lubricants, thereby preventing abrasion and adhesion wear.

Molarious, Korhonen and Ristolainen [27] studied the performance of TiN coated tools during turning with respect to the coating thickness and its composition. As a result of their findings they concluded that there was no direct relation between the coating thickness and the cutting performance, although they reported that some of the thinnest coatings wore out much more rapidly. This result contradicts the findings of reference [23]. The results presented by reference [27] show that the composition of the coating has a more direct influence on performance than the thickness, as better performance was observed with TiN coating having a higher nitrogen content. These results are somewhat different from those reported by the same author in another study and may be due to the different processing parameters used.

In another study Soliman and Abuzeid [28] compared the turning performance of tools coated with 5μ m thick TiN layer. They found that for the same cutting conditions, the TiN coated tools gave a tool life which was 4 times higher than the uncoated tools.

Wallen and Hogmark [29] used the pin on disk wear test to study the wear behaviour of TiN coating. Their results suggest that the wear rate and friction coefficient of TiN nitride is relatively insensitive to different grades of high speed steel material, counterbody temperature and contact mode(intermittent or continuous). The wear rate is primarily affected by the relative speed between the pin and the disk. Scanning Electron Microscope (SEM) analysis of the worn pins showed that adhesion is the primary wear mechanism which affects the pin material, irrespective of the normal load, the counterbody temperature and the contact mode.

The above review shows that extensive research has been carried out by various authors to develop new coating techniques and evaluate their performance using various criteria. In line with the continuing efforts of developing novel coating techniques, a modified PVD multilayer TiN coating technique was used to coat M_7 HSS drill bits as reported by Yilbas et al [2], in which the TiN coat was sputter deposited on the substrate at 260 °C by a dc magnetron source in an argon atmosphere. Plasma nitriding was also done prior to the coating process to obtain an intermediate nitride layer. A multilayer TiN film with a thickness in the range of 2-4μm was obtained. This modified coating technique is expected to improve the machining performance of the drill bits. These drills are the subject of this research. The performance of these twist drills will be evaluated and compared with that of conventional, or commercial, TiN coated twist drills.

Chapter 3

EXPERIMENTAL SETUP AND PROCEDURE

This chapter covers the design and the experimental work performed to generate the data required for evaluating the performance of a new (experimental) TiN coated 1/4 inch (6.35 mm) diameter twist drill and comparing it with the performance of a conventional or commercial TiN coated twist drill. The performance criteria used to evaluate the two types of twist drills are the drilling thrust force and torque, the drill flank wear, the wear patterns on the flank face and the chisel edge of the drill, and the surface roughness of the drilled holes.

Two sets of drilling experiments were performed. In the first set, factorial design drilling experiments were performed to determine the main effects of the process variables on the drill thrust force and torque. The drilling operation process variables or the controllable factors were cutting speed, feed rate, and the method of tool coating. In the second set of experiments each of the drill bits used in the first set were further subjected to machining 20 more holes so as to determine the effect of machining time on the drilling thrust force, torque. drill flank wear and drilled hole surface roughness.

3.1 The Drilling Experiment Setup

The drilling experiments were conducted on a *Bridgeport*^{R} series-II NC milling machine. A schematic diagram of the experimental setup consisting of the test machine and data acquisition instrumentation is shown in figure 3.1. The machine was programmed to drill holes at the selected cutting conditions. Numerical Control part

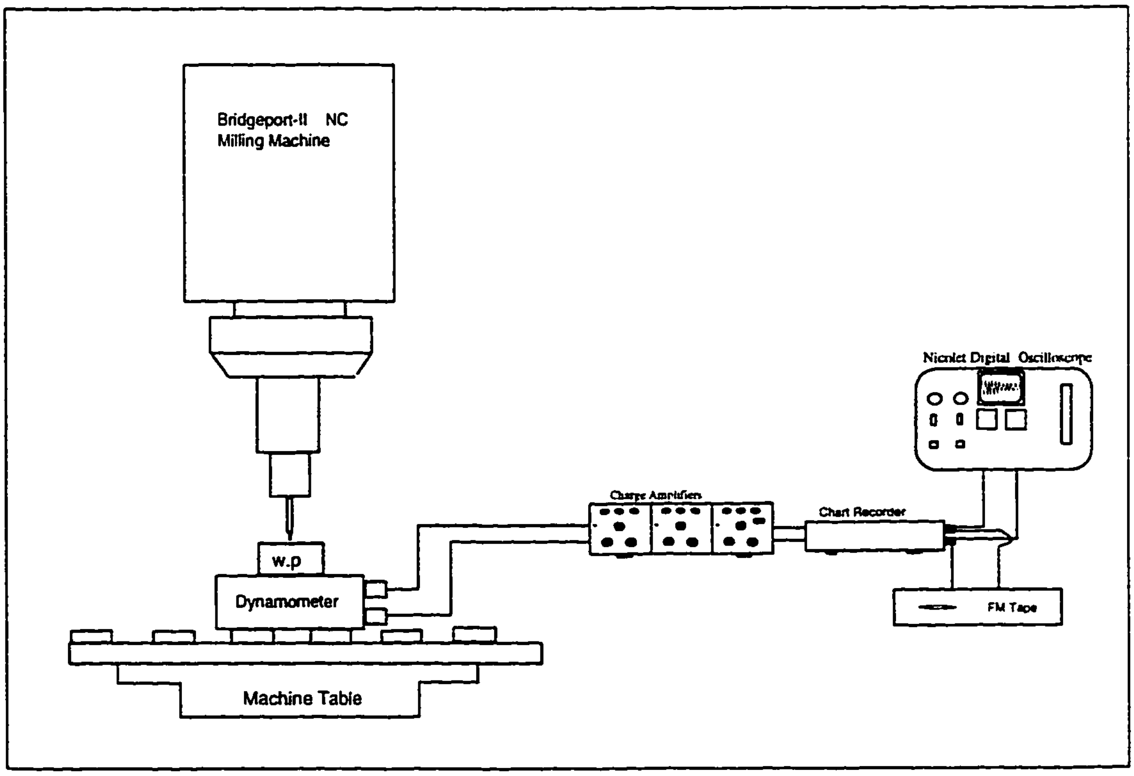

Figure 3.1: Schematic Diagram of the Experimental Setup

programmes were developed for individual test conditions and were fed to the machine via a punched tape. The program consisted of two basic operations namely a simple linear traversing motion of the machine table in the x and y directions for coordinate positioning and a feed motion in the z direction at the specified feed rate for actual cutting. The rotary motion is given to the tool from the machine spindle. The workpiece material chosen for the experiments was AISI 303 stainless steel, having an average hardness of 265HB. The nominal composition of the work material by weight is 0.15%C, 2.0%Mn, 1.0%Si, 17-19%Cr, 8-10%Ni, 0.2%P, 0.15%S, 0.6%Mo, and Fe as the balance. The workpiece was a short cylindrical billet with 3/4 inch(19.05mm) in diameter and 1.0 inch(25.4mm) in length. The holes are drilled in the center of the billets parallel to their axis.

The first set of drill bits used were TiN coated by a new PVD coating technique as reported in [2]. The second set of drill bits are also TiN coated HSS drills made by a major drill bit manufacturer and purchased from a local hardware store. The performance of the former set of drill bits will be compared with that of the later set. The base material of both types of drills is AISI M_7 high speed steel grade. Both types of drill bits were 1/4 inch (6.35 mm) in diameter and 118° point angle. The length of the new and commercial drills are 101 mm and 159 mm respectively. Although the length's of the two types of drill bits were not the same, they were fitted in the drilling chucks in such a way as to have the same overhang length. The nominal composition of the tool base material by weight is $0.95-1.05$%C, 1.0%Co. $3.5-4.5$%Cr, $8.2-9.2$%Mo, $1.7-2.2$%V, 1.75%W and the balance being Fe. Due to the availability of only a small number of experimental drills the study was restricted to investigating the effect of the cutting speed, feed rate and the method of coating only. All other variables were kept constant throughout the experiments.

A two-level-three-variable(2^3) factorial design was used to study the effects of the cutting speed, feed rate and the method of the TiN coating on the response variables of the drilling thrust force and torque. The design matrix for conducting the drilling experiments is shown in Table 3.1.

Table 3.1: The Design Matrix for the Drilling Experiments

Test No.	Run Order	Speed(rpm)	Feed(mm/rev)	Drill Type
1	5	300	0.05	Commercial
2	6	300	0.05	Commercial
3	7	600	0.05	Commercial
4	8	600	0.05	Commercial
5	13	300	0.10	Commercial
6	14	300	0.10	Commercial
7	1	600	0.10	Commercial
8	2	600	0.10	Commercial
9	15	300	0.05	Experimental
10	16	300	0.05	Experimental
11	9	600	0.05	Experimental
12	10	600	0.05	Experimental
13	3	300	0.10	Experimental
14	4	300	0.10	Experimental
15	11	600	0.10	Experimental
16	12	600	0.10	Experimental
Drill dia = 1/4 inch (6.35mm)				

The levels of the main factors or process parameters were selected to correspond to those recommended by the commercial drill manufacturer for dry cutting. A new drill bit was used for each test run and each test was replicated. All drilling operations were performed dry with no coolant supply.

3.2 Experimental Procedure

3.2.1 Measurement of the Drilling Thrust Force and Torque

The drilling thrust force and torque were measured with a four component Kistler^R drill dynamometer. The dynamometer was calibrated before conducting the drilling tests, using a specially designed fixture for its applicable ranges of thrust force and torque. The drilling thrust force and torque output signals from the dynamometer were amplified using charge amplifiers. A chart recorder was connected to the charge amplifier for recording the signals. The calibration data for the thrust force and the torque is shown in Table 3.2 and Table 3.3 respectively and the calibration curves for the drilling thrust force and torque are shown in Figure 3.2 and Figure 3.3, respectively.

Table 3.2: Calibration Data for Drilling Thrust Force

S.No.	Applied Thrust(N)	Instrument† Output pC‡
1	97.9	90.0
2	195.8	178.0
3	293.7	245.0
4	391.6	316.0
5	489.5	384.9
6	587.4	463.0
7	685.3	530.0
8	783.2	600.0
9	881.1	672.0
10	979.0	741.0
11	1076.9	815.8
12	1174.8	887.4
13	1272.7	958.9
14	1370.6	1030.5
15	1468.5	1102.1
16	1566.4	1173.7
17	1664.3	1245.3
18	1762.2	1316.9
19	1860.0	1388.5
20	1957.9	1460.1
21	2055.8	1531.7
22	2153.7	1603.3
23	2251.6	1674.9
24	2349.5	1746.5
25	2447.4	1818.0

†=Charge amplifier; ‡pC=pico Coulombs

Table 3.3: Calibration Data for Drilling Torque

S.No.	Applied Torque(N.m)	Instrument† Output(pC‡)
1	5.5	13.3
2	11.1	26.3
3	16.6	40.1
4	22.1	54.3
5	27.7	68.2
6	33.2	82.6
7	38.7	97.2
8	44.3	113.2
9	49.8	128.6
10	55.3	142.5

†=Charge amplifier; ‡pC=pico Coulombs

The values of the drilling thrust force and torque corresponding to each drilling operation test condition were obtained from their respective calibration charts. Along with the thrust force, the drilling torque signals were simultaneously recorded on the chart recorder. Typical plots from the chart recorder for the drilling thrust force and the drilling torque are shown in Figure 3.4 and Figure 3.5 respectively. Since each of the drilling thrust force recorded signals shows a profile similar to that in Figure 3.4, five values of the force are obtained from each force profile and listed in columns 2 to 5 of Tables 4.5, 4.6, 4.7, 4.8 in Chapter 4. These are F_{entry}, F_{exit}, Fss_u, Fss and Fss_l. The force F_{entry} is the value of the thrust force at the point of initial penetration of the drill into the workpiece and F_{exit} is the thrust force at the point where the drill exists the workpiece. The force Fss, Fss_u and Fss_l are the values of the thrust force at the steady state or full penetration stage of drilling and they indicate respectively the average, the maximum and the minimum values of

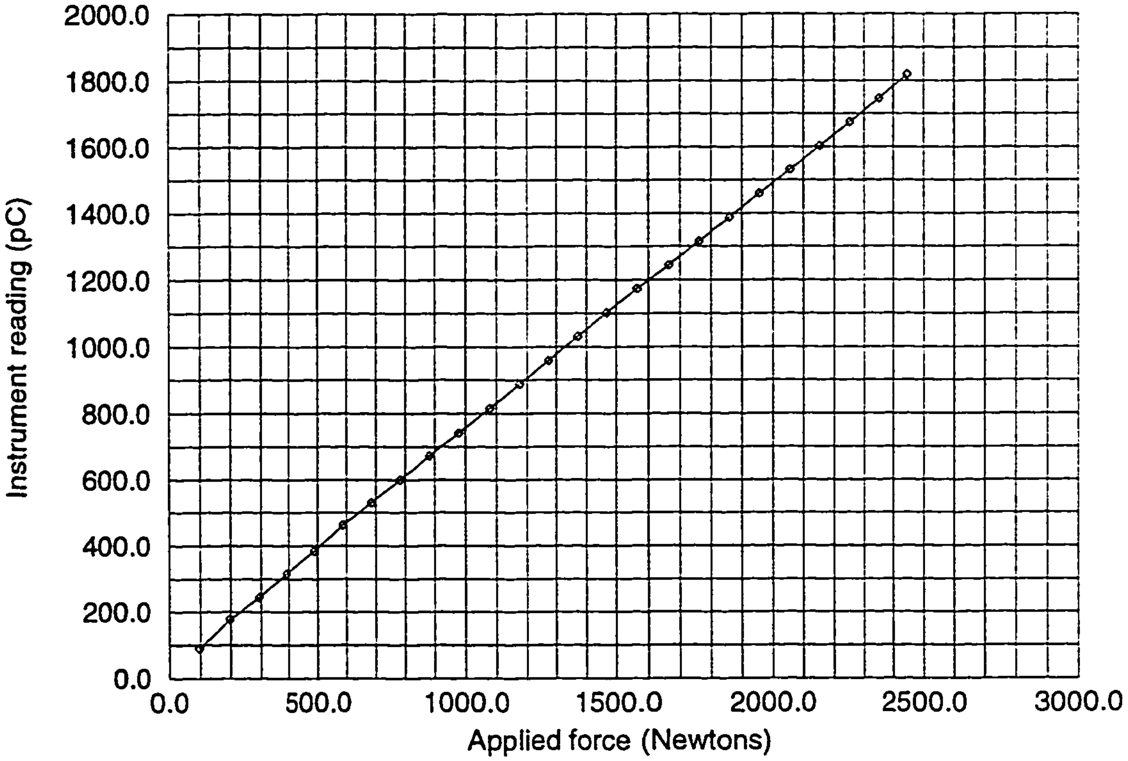

Figure 3.2: Calibration Curve for the Kistler Drilling Dynamometer Thrust Force

the fluctuating steady state stage force signal at a certain depth of the hole. The same convention has been followed for the drilling torque to obtain the five torque values named T_{entry}, T_{exit}, Tss, Tss_u, and Tss_l.

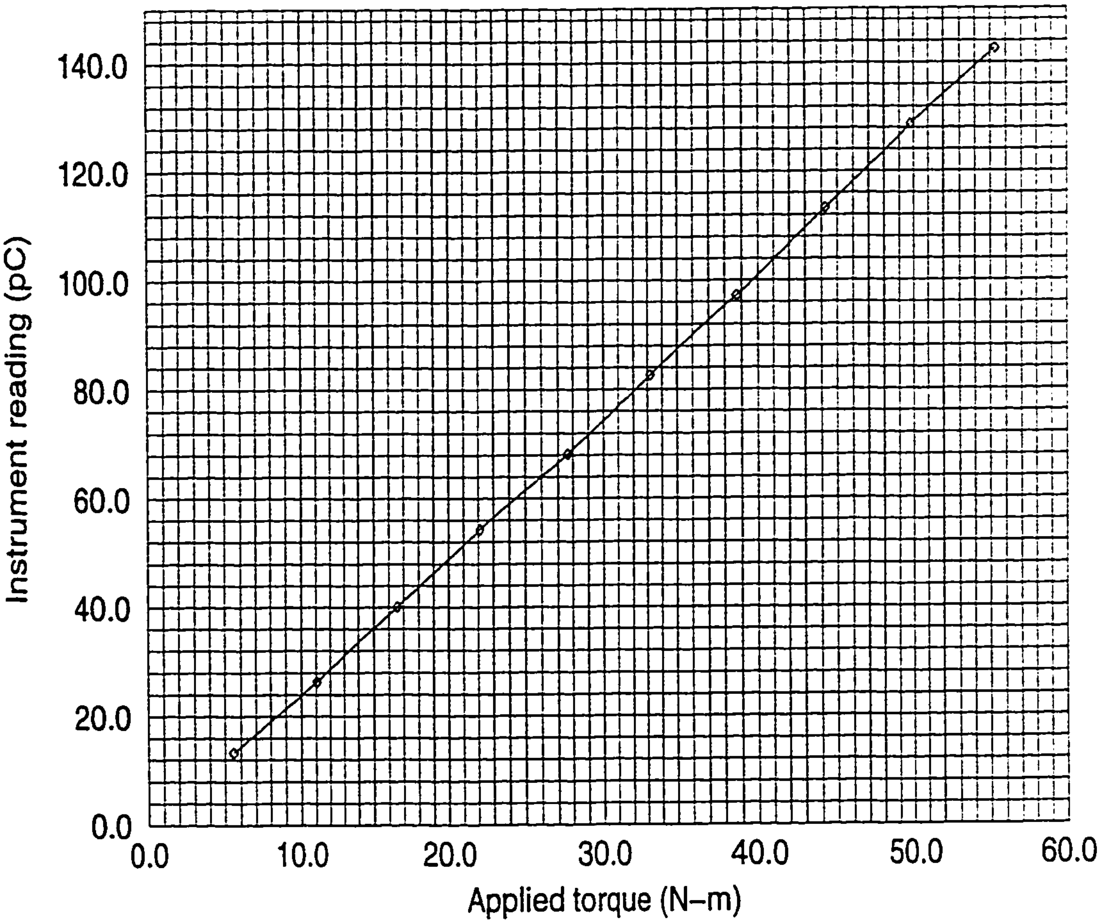

Figure 3.3: Calibration curve for Kistler drilling dynamometer torque

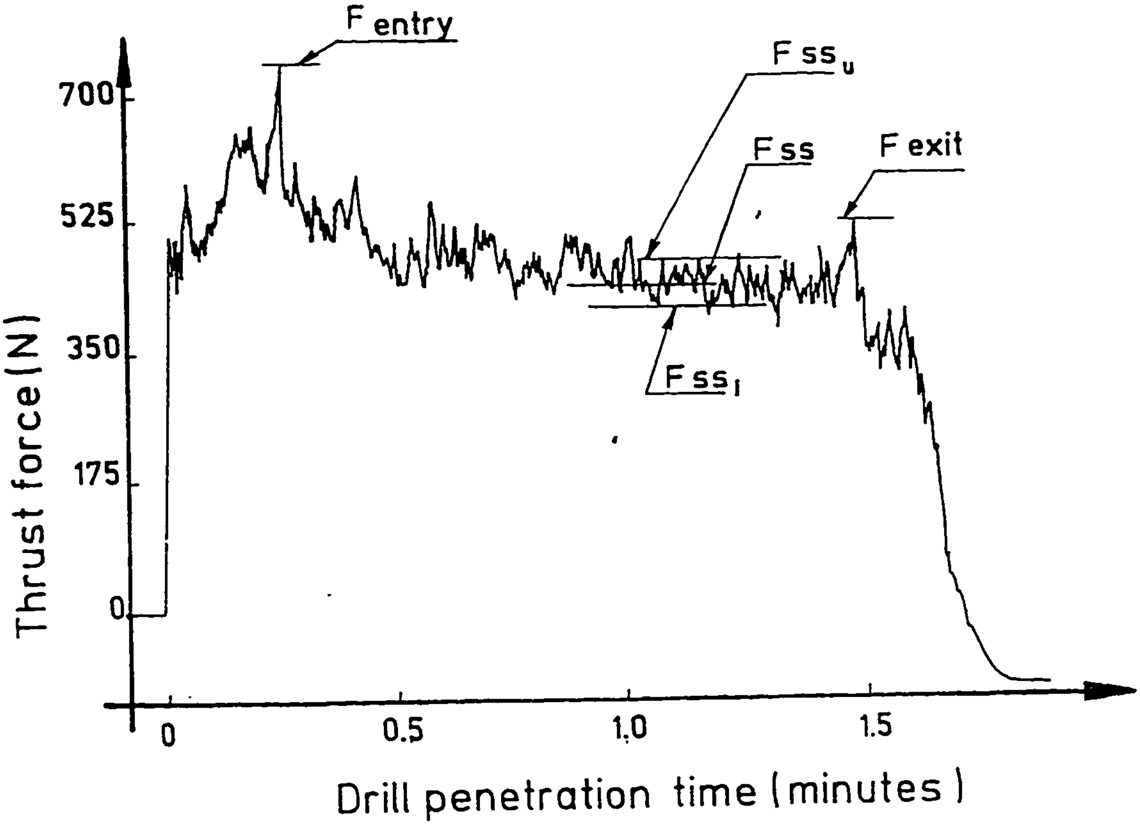

Figure 3.4: Typical Signal of the Drilling Thrust Force Obtained from the Chart Recorder

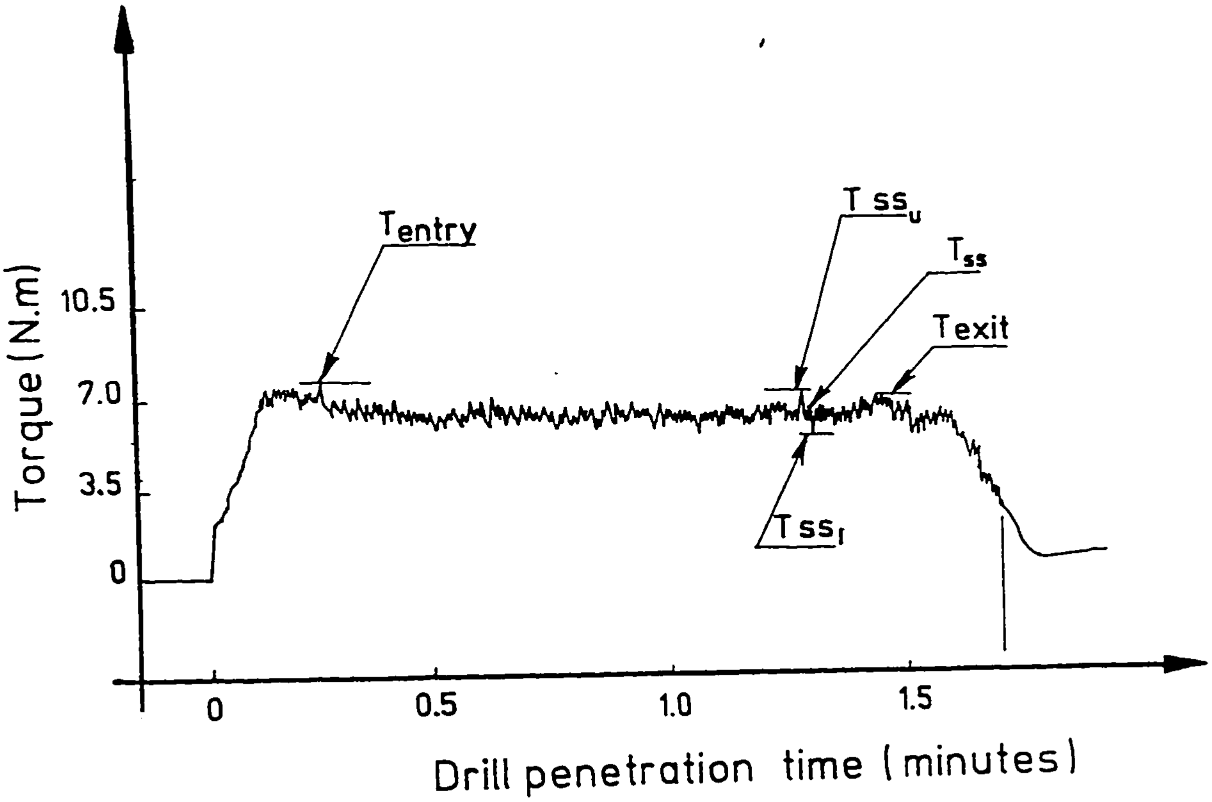

Figure 3.5: Typical Signal of the Drilling Torque Obtained from the Chart Recorder

3.2.2 Measurement of Drill Flank Wear by an Optical Method

For each of the test conditions of the Titanium Nitride (TiN) coated drills indicated in Table 3.1, the width of the wear land on the flank face of the drill was measured using a Leitz universal toolmakers microscope. Wear marks were measured at three different locations A, B, and C on the edge of the flank as shown in figure 3.6. Point A corresponds to the maximum width of wear land 'VB' on the edge of the flank face in mm, while point B corresponds to the wear land width at approximate centre of the cutting edge on the flank face, and point C corresponds to the wear land width at a location which is 0.5mm distance from the intersection point of the chisel edge and the cutting edge. Because of very small increments in the wear marks, the wear was measured for each drill at an interval of three drilled holes up to hole number twenty one.

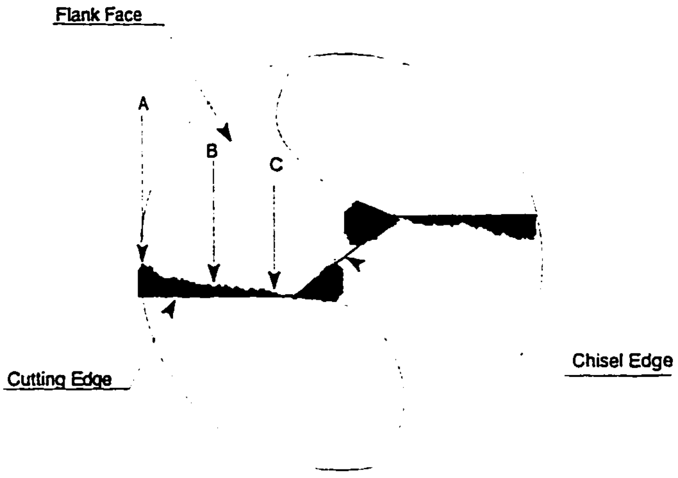

Figure 3.6: Measured Wear Regions of the Twist Drills

3.2.3 Wear Pattern Measurements by Micro-PIXE Technique

The underlying principle of micro-PIXE technique is that a proton beam of 2-4 MeV energy is used to bombard the sample surface being examined, and excite the electrons of the innermost shells of the atoms in the sample. The characteristic X-ray yields emitted from the sample are used to identify and quantify the elemental sample composition. Scanning a fine focused beam over the sample surface and correlating the detected characteristic X-ray quants with the beam position allows the generation of elemental distribution maps. The maps thus constructed are used for identifying the distribution of various trace elements in a sample. The technique is known as X-ray mapping. For calibration purposes the values of the x-ray detector window thickness and the crystal thickness provided by the manufacturer were used, which are usually not very accurate. For this reason an error of ± 5% is assumed in the energy range of 5KeV to 10keV. This error increases to ± 10% for elements above 10KeV energy levels, while on the lower side of the energy spectrum error may exceed ± 50%. In this experiment a proton(H^+) beam of 2.5MeV from the KFUPM[1] tendetron nuclear accelerator[30] was used to study the worn drill bits after drilling twentyone holes, for the presence of trace amounts of work or tool materials on the surface of the flank and the chisel edges. By comparing the ratio of the measured yields from Ti(coat) and Fe(underlying tool base) with the ratio calculated using the PIXE analysis software package 'GUPIX' [31], the TiN coating thicknesses were determined for several locations on the flank face and the chisel edge.

---

[1] King Fahd University of Petroleum and Minerals

3.2.4 Measurement of Drilled Hole Surface Roughness

In order to measure the surface roughness of the drilled holes, each machined specimen was parted along the center line to expose the machined surface. One of the resulting two surfaces was chosen at random to measure the roughness profile. A Surtronic-3P roughness measuring instrument manufactured by Taylor Hobson was used for this purpose. A cutoff length of 2.5 mm was selected. The probe was arranged to traverse along the direction of the feed and perpendicular to the feed marks. Three readings of the roughness profile center line average, 'R_a' values in micro meters were recorded for each hole.

Chapter 4

RESULTS AND DISCUSSION

4.1 Effect of the Process Parameters on the Drilling Thrust Force and Torque

The steady state drilling thrust force (Fss) and the steady state torque (Tss) are obtained from the respective force and torque signals recorded in section 3.2.1 for the replicated 2^3 factorial design test conditions listed in Table 3.1. The steady state values of the thrust forces from the drilling tests of the new TiN coated drills(experimental drills) and the commercially purchased TiN coated drills(commercial drills) are listed in Table 4.1. Since both types of drill bits are of the same geometry and were subjected to the same cutting conditions, any observed differences in the thrust force values of the two types of drills could be attributed to the difference in the coating procedure. The steady state drilling torque corresponding to the replicated tests of the design matrix of Table 3.1 are listed in Table 4.2. The data in Table 4.1 and the data in Table 4.2 are used to evaluate the effects of the major

Table 4.1: The Steady State Drilling Thrust Force Values of The Experimental and Commercial TiN Coated Drills at the Replicated Test Conditions

Experimental Drill			
Spindle Speed(rpm)	Feed Rate(mm/rev)	Fss1(N)	Fss2 (N)
300	0.05	427	449
600	0.05	330	360
300	0.10	1470	1481
600	0.10	1308	1362
Commercial Drill			
Spindle Speed(rpm)	Feed Rate(mm/rev)	Fss1(N)	Fss2 (N)
300	0.05	406	416
600	0.05	338	342
300	0.10	1578	1632
600	0.10	1605	1618
Fss1= steady state thrust Force for first run Fss2= steady state thrust Force for second run			

Table 4.2: The Steady State Drilling Torque Values of The Experimental and Commercial TiN Coated Drills at the Replicated Test Conditions

Experimental Drill,			
Spindle Speed (rpm)	Feed Rate(mm/rev)	Tss1(N.m)	Tss2(N.m)
300	0.05	5.65	5.96
600	0.05	4.54	4.72
300	0.10	7.01	7.07
600	0.10	6.39	6.83
Commercial Drill			
Spindle Speed (rpm)	Feed Rate(mm/rev)	Tss1(N.m)	Tss2(N.m)
300	0.05	4.54	4.85
600	0.05	4.60	5.12
300	0.10	4.97	5.25
600	0.10	8.68	9.79
Tss1= steady state torque for first run Tss2= steady state torque for second run			

test factors, i.e. the cutting speed and the feed rate, on the steady state values of drilling thrust forces and torques respectively of the two types of TiN coated twist drills.

The 95% confidence intervals of the mean response of the main effects of cutting speed, and feed rate and their interaction on the steady state thrust force(Fss) of the experimental and the commercial drill were estimated by the method described in reference [32], for the range of speed and feed rate given in Table 3.1 from the data in Table 4.1. The results are shown in Table 4.3.

Table 4.3: Calculated Effects and Standard Errors for the Drilling Thrust Force for the (a)Experimental and (b)Commercial Drill Bits.

(a) Experimental Drill, (6.35mm dia)	
Effect	Estimate(N) ± Standard error
Average	898.84± 8.26
Main effects	
Speed(rpm)	−116.53 ± 16.51
Feed(mm/rev)	1013.94 ± 16.51
Two factor interaction	
Speed x Feed	−23.56 ± 16.51

(b) Commercial Drill, (6.35mm dia)	
Average	992.357± 7.11
Main effects	
Speed(rpm)	−32.04 ± 14.22
Feed(mm/rev)	1232.64 ± 14.22
Two factor interaction	
Speed x Feed	38.70 ± 14.22

Likewise, the 95% confidence intervals of the main effects of speed and feed rate and their interaction on the drilling torque for the experimental and the commercial drills estimated from the factorial design data of Table 4.2 are listed in Table 4.4. The confidence intervals of the mean response, main effects and the two variable interactions of Table 4.3 and Table 4.4 are used to judge the statistical significance of variable effects on the drilling thrust force and torque of the experimental and the commercial drills. The null hypothesis (Ho: true mean effect is zero) is rejected if the confidence interval values are strictly either positive or negative. From Table

Table 4.4: Calculated Main Effects and their Interaction for the Drilling Torque of (a)Experimental and (b)Commercial Drill Bits.

(a) Experimental Drill, (6.35mm dia)	
Effect	Estimate (N.m)± Standard error
Average	6.02± 0.07
Main effects	
Speed(rpm)	-0.80 ± 0.14
Feed(mm/rev)	1.60 ± 0.14
Two factor interaction	
SpeedxFeed	0.37 ± 0.14
(b) Commercial Drill, (6.35mm dia)	
Average	5.92± 0.14
Main effects	
Speed(rpm)	2.05 ± 0.29
Feed(mm/rev)	2.49 ± 0.29
Two factor interaction	
SpeedxFeed	2.08 ± 0.29

4.3, it appears that the main factors as well as their interaction have a statistically significant effect on the thrust force for both types of drills. The main effect of a variable can be individually interpreted only if there is no evidence of interaction with other variables[33].

In Table 4.3 there appears to be a significant speed and feed rate effects on thrust force for the experimental drill. But as the feed rate interacts with the speed, (the two factor interaction is -23.56 ± 16.51), no statement can be made about the effect of speed or feed rate alone. The effect of speed and feed interaction is to decrease the thrust force of the experimental drill. However, contrary to the experimental drill, for the commercial drill, the two factor interaction of speed and feed is positive, i.e. they tend to increase the thrust force. There is a very high positive effect of the feed rate on the thrust force. The effect of speed is negative and its magnitude is relatively small compared to the effect of feed and the two factor interaction of speed and feed.

It is observed from Table 4.4 that, for the drilling torque, the main effects of cutting speed and feed rate as well as the effect of their two factor interaction are all significant at the 95% confidence level as their intervals do not include zero for both the experimental drill as well as the commercial drill. Although the individual effect of speed is negative for the experimental drill and positive for the commercial drill, the effect of their interaction is positive for both types of drills. This means that an increase in the cutting speed as well as the feed rate increases the drilling torque.

4.2 Development of Thrust Force and Torque Models

For the prediction of the drilling thrust force and torque at different cutting conditions, a response surface model was postulated for the torque and the thrust force to fit the data obtained from the factorial experiments listed in Table 4.1 and Table 4.2. This model was selected because it represented the best fit to the data obtained from the factorial experiments. The general form of such a model is given by the following equation :

$$Response = b_o + b_1N + b_2F + b_1b_2NF............ \qquad (4.1)$$

where bo, b1 and b2 are constants to be determined. N is the spindle speed in rpm and F is the feed rate in mm/rev. The use of this model is limited, within the range of cutting speeds and feed rates used in the experiments. Multiple regression analysis was used to estimate the constants in the above models. The Statgraphics [34] software was used for fitting these models. The resulting model of the steady state thrust force(Fss) in Newtons for the experimental drills and the commercial drills are:

$$Fss(experimental) = 898.844 - 58.27(N) + 506.97(F) - 11.78(N)(F)..... \qquad (4.2)$$

$$Fss(commercial) = 992.357 - 16.02(N) + 616.32(F) + 19.35(N)(F)..... \qquad (4.3)$$

The R^2 value for the models of equations 4.2 and 4.3 was obtained as 99.895 and 99.947 respectively. The R^2 statistic is a measure of the models overall performance,i.e. it is the percentage of total variability in the data that is accounted for by the model[32]. The R^2 statistic indicates that the model as fitted explains about 99 percent of the variability in Fss. For the above models, two standard error limits of the effect estimates show that, the average effect, the main effects and the interaction effects are all significant at this level. Hence no factor can be removed from the models. The steady state thrust force model for the experimental drill shows that the speed and feed interaction tends to decrease the thrust force, whereas for the commercial drill the speed and feed interaction tends to increase the thrust force, however for both the drills the individual effect of feed is to increase the thrust force. This implies that increasing the cutting speed decreases the thrust force for the experimental drill. The reason may be due to elimination of built-up-edge at the higher level of cutting speed.

The following similar models were developed for the steady state torque in Newton-meter:

$$Tss(experimental) = 6.021 - 0.4013(N) + 0.804(F) + 0.186(N)(F).... \qquad (4.4)$$

$$Tss(commercial) = 5.925 + 1.023(N) + 1.248(F) + 19.35(N)(F)...... \qquad (4.5)$$

The R^2 value for the models in equations 4.4 and 4.5 was obtained as 97.64 and 97.65 respectively. The R^2 statistic indicates that the model as fitted explains about 98 percent of the variability in the steady state torque "Tss", for both the drills.

The steady state torque models for both the experimental and commercial drills show that the interaction of the speed and the feed rate is to increase the torque, however the individual effect of speed for the experimental drill is to decrease the steady state torque. The reason could be that at the higher level of cutting speed there is a reduced tendency of built-up-edge formation for the experimental drill as compared to the commercial drill. It is important to mention here that the regression models developed for the thrust force and the drilling torque are valid only within the range of the cutting speeds and feeds employed. Furthermore, the data for the drilling thrust force and torque models was obtained from a small sample(four data points with one replication each) hence these models cannot be generalized.

4.3 Effect of Machining Time on Thrust Force and Torque

After the completion of the first set of experiments, which were conducted to obtain the effects of the cutting parameters on the drilling thrust and torque, the same drills were further subjected to machining tests at their respective cutting speeds and feed rates as described in section 3.2.1 to determine the effect of machining time(or the number of drilled holes) on the thrust force, drilling torque, the flank wear, the wear patterns of the drills and the drilled hole surface roughness.

The thrust force data resulting from these tests are listed in Table 4.5 for the experimental drills and Table 4.6 for the commercial drills. The digitized drilling torque values at different cutting times are shown in Table 4.7 for the experimental drills and Table 4.8 for the commercial drills respectively.

Table 4.5: The Drilling Thrust Force Data for the Experimental Drills at the Given Cutting Conditions

<table>
<tr><th colspan="7">Drilling Thrust Force (N)</th></tr>
<tr><th colspan="7">Speed 300 rpm, Feed 0.05 mm/rev</th></tr>
<tr><th>Hole</th><th>Time(min)</th><th>Fss_u</th><th>Fss_l</th><th>Fss</th><th>F_{entry}</th><th>F_{exit}</th></tr>
<tr><td>1</td><td>1.67</td><td>451.83</td><td>414.10</td><td>427.58</td><td>742.89</td><td>513.82</td></tr>
<tr><td>3</td><td>5.00</td><td>500.34</td><td>325.17</td><td>411.41</td><td>581.19</td><td>527.29</td></tr>
<tr><td>6</td><td>10.02</td><td>513.82</td><td>352.12</td><td>432.97</td><td>581.19</td><td>567.72</td></tr>
<tr><td>9</td><td>15.03</td><td>500.34</td><td>419.49</td><td>459.92</td><td>729.41</td><td>513.82</td></tr>
<tr><td>12</td><td>20.04</td><td>581.19</td><td>419.49</td><td>459.92</td><td>796.79</td><td>621.61</td></tr>
<tr><td>15</td><td>25.05</td><td>688.99</td><td>419.49</td><td>462.61</td><td>891.11</td><td>608.14</td></tr>
<tr><td>18</td><td>30.06</td><td>635.09</td><td>446.44</td><td>468.00</td><td>850.68</td><td>715.94</td></tr>
<tr><td>21</td><td>35.07</td><td>688.99</td><td>486.87</td><td>500.34</td><td>837.21</td><td>680.90</td></tr>
<tr><th colspan="7">Speed 300 rpm, Feed 0.10 mm/rev</th></tr>
<tr><th>Hole</th><th>Time(min)</th><th>Fss_u</th><th>Fss_l</th><th>Fss</th><th>F_{entry}</th><th>F_{exit}</th></tr>
<tr><td>1</td><td>0.83</td><td>1524.42</td><td>1416.62</td><td>1470.52</td><td>1551.37</td><td>1524.42</td></tr>
<tr><td>3</td><td>2.50</td><td>1632.22</td><td>1483.99</td><td>1564.84</td><td>1691.50</td><td>1564.84</td></tr>
<tr><td>6</td><td>5.00</td><td>1659.17</td><td>1470.52</td><td>1578.32</td><td>1793.91</td><td>1659.17</td></tr>
<tr><td>9</td><td>7.47</td><td>1955.61</td><td>1645.69</td><td>1713.06</td><td>2165.81</td><td>1632.22</td></tr>
<tr><td>12</td><td>9.96</td><td>1982.56</td><td>1793.91</td><td>1847.81</td><td>2300.56</td><td>1766.96</td></tr>
<tr><td>15</td><td>12.45</td><td>1982.56</td><td>1740.01</td><td>1847.81</td><td>2359.85</td><td>1653.78</td></tr>
<tr><td>18</td><td>14.94</td><td>2036.46</td><td>1820.86</td><td>1928.66</td><td>2117.31</td><td>1928.66</td></tr>
<tr><td>21</td><td>17.43</td><td>2063.41</td><td>1766.96</td><td>1928.66</td><td>2467.65</td><td>2036.46</td></tr>
<tr><th colspan="7">Speed 600rpm, Feed 0.05 mm/rev</th></tr>
<tr><th>Hole</th><th>Time(min)</th><th>Fss_u</th><th>Fss_l</th><th>Fss</th><th>F_{entry}</th><th>F_{exit}</th></tr>
<tr><td>1</td><td>0.83</td><td>392.54</td><td>257.80</td><td>330.56</td><td>473.39</td><td>392.54</td></tr>
<tr><td>3</td><td>2.50</td><td>406.02</td><td>284.75</td><td>338.65</td><td>513.82</td><td>473.39</td></tr>
<tr><td>6</td><td>5.00</td><td>406.02</td><td>271.27</td><td>333.26</td><td>478.78</td><td>527.29</td></tr>
<tr><td>9</td><td>7.47</td><td>419.49</td><td>271.27</td><td>344.04</td><td>489.56</td><td>648.56</td></tr>
<tr><td>12</td><td>9.96</td><td>449.14</td><td>284.75</td><td>349.43</td><td>548.85</td><td>473.39</td></tr>
<tr><td>15</td><td>12.45</td><td>446.44</td><td>284.75</td><td>352.12</td><td>527.29</td><td>500.34</td></tr>
<tr><td>18</td><td>14.94</td><td>446.44</td><td>279.36</td><td>360.21</td><td>468.00</td><td>473.39</td></tr>
<tr><td>21</td><td>17.43</td><td>451.83</td><td>290.14</td><td>373.68</td><td>500.34</td><td>581.19</td></tr>
<tr><th colspan="7">Speed 600rpm, Feed 0.10 mm/rev</th></tr>
<tr><th>Hole</th><th>Time(min)</th><th>Fss_u</th><th>Fss_l</th><th>Fss</th><th>F_{entry}</th><th>F_{exit}</th></tr>
<tr><td>1</td><td>0.42</td><td>1389.67</td><td>1147.13</td><td>1308.82</td><td>1470.52</td><td>1362.72</td></tr>
<tr><td>3</td><td>1.25</td><td>1470.52</td><td>1281.87</td><td>1376.20</td><td>1443.57</td><td>1551.37</td></tr>
<tr><td>6</td><td>2.50</td><td>1524.42</td><td>1335.77</td><td>1443.57</td><td>1659.17</td><td>1659.17</td></tr>
<tr><td>9</td><td>3.78</td><td>1659.17</td><td>1389.67</td><td>1481.30</td><td>1820.86</td><td>1815.47</td></tr>
<tr><td>12</td><td>5.04</td><td>1578.32</td><td>1362.72</td><td>1454.35</td><td>1659.17</td><td>1686.12</td></tr>
<tr><td>15</td><td>6.30</td><td>1713.06</td><td>1093.23</td><td>1556.76</td><td>1955.61</td><td>2009.51</td></tr>
</table>

Table 4.6: Drilling Thrust Force Data for the Commercial Drills at the Given Cutting Conditions

Drilling Thrust Force (N)						
Speed 300 rpm, Feed 0.05 mm/rev						
Hole	Time(min)	Fss_u	Fss_l	Fss	F_{entry}	F_{exit}
1	1.67	473.39	365.60	406.02	554.24	432.97
3	5.00	419.49	279.36	387.15	486.87	635.09
6	10.02	459.92	298.22	397.93	513.82	694.38
9	15.03	476.09	282.05	419.49	521.90	594.66
12	20.04	473.39	284.75	416.80	554.24	662.04
15	25.05	486.87	284.75	408.71	554.24	688.99
18	30.06	494.95	279.36	419.49	540.77	608.14
21	35.07	505.73	284.75	414.10	513.82	635.09
Speed 300 rpm, Feed 0.10 mm/rev						
Hole	Time(min)	Fss_u	Fss_l	Fss	F_{entry}	F_{exit}
1	0.83	1901.71	1254.92	1578.32	2138.86	2020.29
3	2.50	1901.71	1254.92	1621.44	2171.20	1977.17
6	5.00	1815.47	1254.92	1643.00	2128.08	1955.61
9	7.47	1793.91	1362.72	1664.56	2063.41	1837.03
12	9.96	2009.51	1254.92	1686.11	2181.98	2009.51
15	12.45	1987.95	1847.81	1707.67	2117.31	2084.97
18	14.94	1966.39	1362.72	1686.11	2181.98	1880.15
21	17.43	2009.51	1362.72	1675.34	2279.00	2138.86
Speed 600 rpm, Feed 0.05 mm/rev						
Hole	Time(min)	Fss_u	Fss_l	Fss	F_{entry}	F_{exit}
1	0.83	392.54	244.32	338.65	432.97	298.22
3	2.50	392.54	311.70	344.04	473.39	322.48
6	5.00	392.54	230.85	338.65	486.87	284.75
9	7.47	432.97	230.85	352.12	494.95	344.04
12	9.96	441.05	257.80	360.21	486.87	379.07
15	12.45	446.44	311.70	365.60	473.39	635.09
18	14.94	441.05	298.22	357.51	513.82	581.19
21	17.43	446.44	306.31	370.98	473.39	715.94
Speed 600 rpm, Feed 0.10 mm/rev						
Hole	Time(min)	Fss_u	Fss_l	Fss	F_{entry}	F_{exit}
1	0.42	1659.17	1578.32	1605.27	1632.22	1726.54
3	1.25	1645.69	1524.42	1548.67	1659.17	1713.06
6	2.50	1686.11	1551.37	1618.74	1605.27	1901.71
9	3.78	1686.11	1578.32	1578.32	1691.50	1740.01
12	5.04	1691.50	1578.32	1632.22	1713.06	1793.91
15	6.30	1659.17	1578.32	1605.27	1686.11	2090.36
18	7.56	1524.42	1389.67	1578.32	1578.32	2009.51
21	8.82	1659.17	1524.42	1629.52	1761.57	2117.31

Table 4.7: The Drilling Torque Data for the Experimental Drills at the Given Cutting Conditions

Drilling Torque (N.m)						
Speed 300 rpm, Feed 0.05 mm/rev						
Hole	Time(min)	Tss_u	Tss_l	Tss	T_{entry}	T_{exit}
1	1.67	6.70	5.28	5.65	7.14	6.39
3	5.00	5.47	4.35	4.97	5.77	9.18
6	10.02	6.70	4.85	5.16	6.08	10.41
9	15.03	6.08	4.85	5.34	5.96	8.56
12	20.04	6.45	5.47	5.53	7.32	9.42
15	25.05	6.95	5.96	6.08	7.07	9.79
18	30.06	6.70	5.84	6.08	7.32	12.27
21	35.07	6.70	4.60	6.27	6.21	13.50
Speed 300 rpm, Feed 0.10 mm/rev						
Hole	Time(min)	Tss_u	Tss_l	Tss	T_{entry}	T_{exit}
1	0.83	7.32	6.70	7.01	7.32	8.56
3	2.50	8.00	6.70	6.83	8.06	10.16
6	5.00	7.44	6.70	6.95	8.00	13.87
9	7.47	7.51	6.70	7.26	7.32	14.18
12	9.96	7.63	7.07	7.44	7.94	14.74
15	12.45	7.44	6.70	7.07	7.94	13.50
18	14.94	7.63	5.77	7.32	7.82	15.36
21	17.43	8.06	7.38	7.44	8.56	14.74
Speed 600 rpm, Feed 0.05 mm/rev						
Hole	Time(min)	Tss_u	Tss_l	Tss	T_{entry}	T_{exit}
1	0.83	4.85	4.23	4.54	4.85	5.47
3	2.50	4.85	4.11	4.41	4.85	12.27
6	5.00	4.97	4.23	4.60	5.40	13.87
9	7.47	4.66	3.80	4.41	5.34	11.65
12	9.96	4.60	3.92	4.48	4.85	7.32
15	12.45	6.08	4.23	4.72	6.08	10.41
18	14.94	5.53	4.35	4.85	5.47	9.18
21	17.43	5.53	4.72	4.97	5.47	12.76
Speed 600 rpm, Feed 0.10 mm/rev						
Hole	Time(min)	Tss_u	Tss_l	Tss	T_{entry}	T_{exit}
1	0.42	7.01	6.08	6.39	6.08	8.56
3	1.25	7.01	6.70	6.83	7.01	13.32
6	2.50	7.32	6.08	6.70	6.83	19.07
9	3.78	7.20	6.08	7.07	6.39	18.45
12	5.04	7.32	6.39	6.83	6.70	15.36
15	6.30	7.94	6.08	7.94	8.56	19.32

Table 4.8: The Drilling Torque Data for the Commercial Drills at the Given Cutting Conditions

Drilling Torque (N.m)						
Speed 300 rpm, Feed 0.05 mm/rev						
Hole	Time(min)	Tss_u	Tss_l	Tss	T_{entry}	T_{exit}
1	1.67	4.85	3.61	4.54	4.85	5.47
3	5.00	4.85	4.23	4.54	4.91	12.27
6	10.02	4.54	3.61	4.11	4.23	12.02
9	15.03	4.54	3.73	4.29	4.54	12.33
12	20.04	4.97	3.92	4.48	4.85	10.54
15	25.05	4.85	3.92	4.35	4.85	12.21
18	30.06	4.54	3.92	4.41	4.48	10.10
21	35.07	4.85	4.11	4.29	4.79	11.40
Speed 300 rpm, Feed 0.10 mm/rev						
Hole	Time(min)	Tss_u	Tss_l	Tss	T_{entry}	T_{exit}
1	0.83	5.34	4.23	4.97	5.40	11.96
3	2.50	5.53	4.72	4.97	5.47	16.60
6	5.00	5.59	4.85	5.09	5.65	12.27
9	7.47	5.77	4.85	5.16	5.53	10.41
12	9.96	5.47	4.85	5.22	5.65	11.03
15	12.45	5.47	4.85	5.16	5.47	12.14
18	14.94	5.47	4.85	5.16	5.77	12.27
21	17.43	5.96	5.16	5.34	6.02	14.12
Speed 600 rpm, Feed 0.05 mm/rev						
Hole	Time(min)	Tss_u	Tss_l	Tss	T_{entry}	T_{exit}
1	0.83	5.22	3.92	4.60	4.17	5.16
3	2.50	4.91	4.23	4.54	4.79	8.56
6	5.00	6.08	4.72	4.85	5.47	9.30
9	7.47	5.96	4.72	5.03	5.47	7.63
12	9.96	5.77	4.85	5.16	5.59	6.39
15	12.45	5.34	4.23	5.09	5.34	9.79
18	14.94	5.47	4.23	5.16	5.53	9.30
21	17.43	6.08	4.85	5.47	5.47	10.91
Speed 600 rpm, Feed 0.10 mm/rev						
Hole	Time(min)	Tss_u	Tss_l	Tss	T_{entry}	T_{exit}
1	0.42	8.96	8.19	8.68	8.56	9.92
3	1.25	11.03	9.79	10.16	10.41	12.89
6	2.50	10.41	9.79	10.24	9.92	15.05
9	3.78	10.41	9.92	10.04	9.92	12.89
12	5.04	10.41	9.86	10.23	9.92	13.19
15	6.30	10.41	9.79	10.10	9.48	14.74
18	7.56	9.79	9.18	9.48	9.05	14.12
21	8.82	10.41	9.79	10.10	9.79	14.99

The drilling time 'T' in the second column of Tables 4.5, 4.6, 4.7, and 4.8 is obtained from the following equation:

$$T = (L_w/f) \times (N) \ldots\ldots\ldots\ldots\ldots\ldots \quad (4.6)$$

where T = Time to drill one hole.

L_w = Length of the hole.

f = feed rate.

N = spindle speed in rpm.

The graphs which show the effect of machining time on the steady state drilling thrust force(Fss) of the experimental drill is plotted from the data of Table 4.5 in Figure 4.1, the curves give the variation of thrust force at their respective cutting conditions as a function of drilling time. At the lower level of feed rate of f = 0.05 mm/rev, the thrust force at both speeds of 300 rpm and 600 rpm show a very small rate of increase in value up to the last hole. At the feed rate of f = 0.10 mm/rev, the thrust force curves at the speeds of 300 rpm and 600 rpm show a higher rate of increase compared to f=0.05 mm/rev. The curves at the 300 rpm speed are above those at the 600 rpm speed at both levels of feed rates(ie f = 0.05 mm/rev and f= 0.10 mm/rev). At a given machining time and at both levels of cutting speed(i.e. 300 rpm and 600 rpm) the value of the thrust force at the higher level of feed rate(0.1 mm/rev)is about four times the value of thrust force corresponding to the lower level of feed rate(0.05 mm/rev).

The curves of the steady state thrust force versus the number of drilled holes of the commercial drill are plotted in Figure 4.2 from the respective cutting conditions data in Table 4.6. For both the 0.05 mm/rev and 0.10 mm/rev feed rates, and

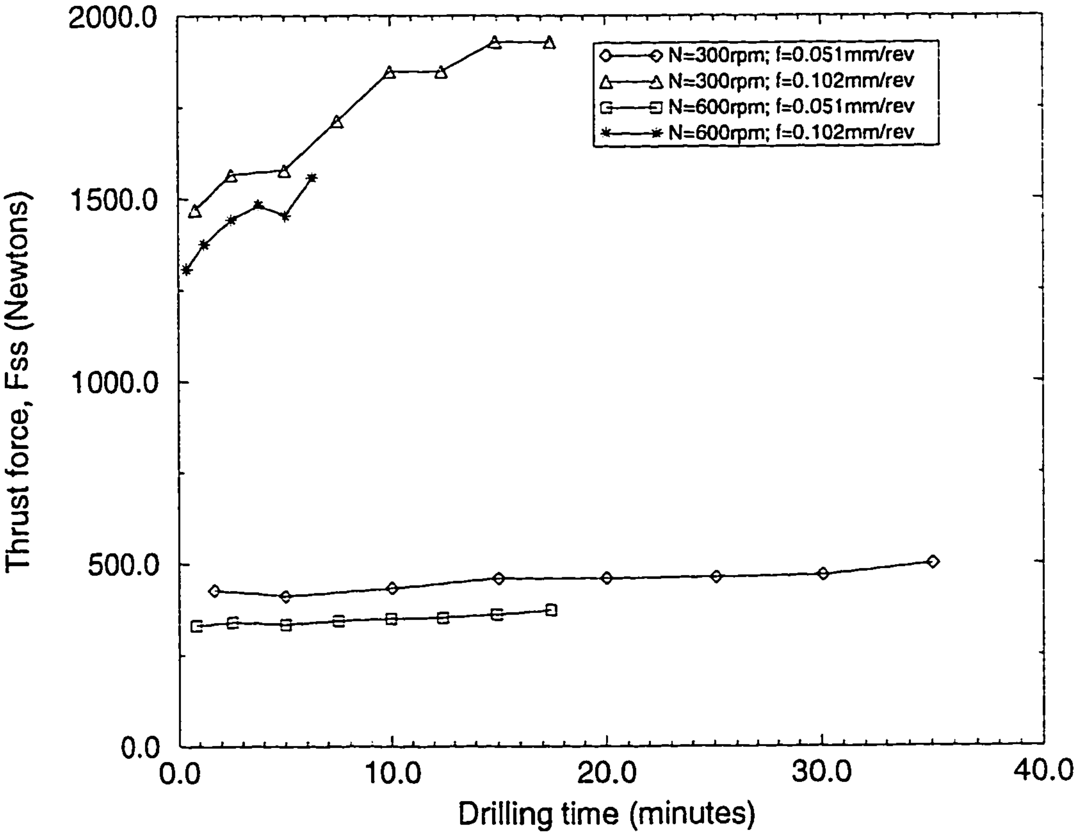

Figure 4.1: Plot of Steady State Thrust Force for the Experimental Drills at Various Cutting Conditions

both levels of speed the thrust force has shown a relatively small increase in value between drilling the third hole and drilling the twenty-first hole. However, for the same rotational speed, the thrust force at a feed rate of 0.10 mm/rev is about four times that of the 0.05 mm/rev. This result is similar to that of the experimental drill shown in Figure 4.1. The increase in the thrust force with the increase in feed is attributed to strain rate effect, as the increased feed rate tends to increase the strain

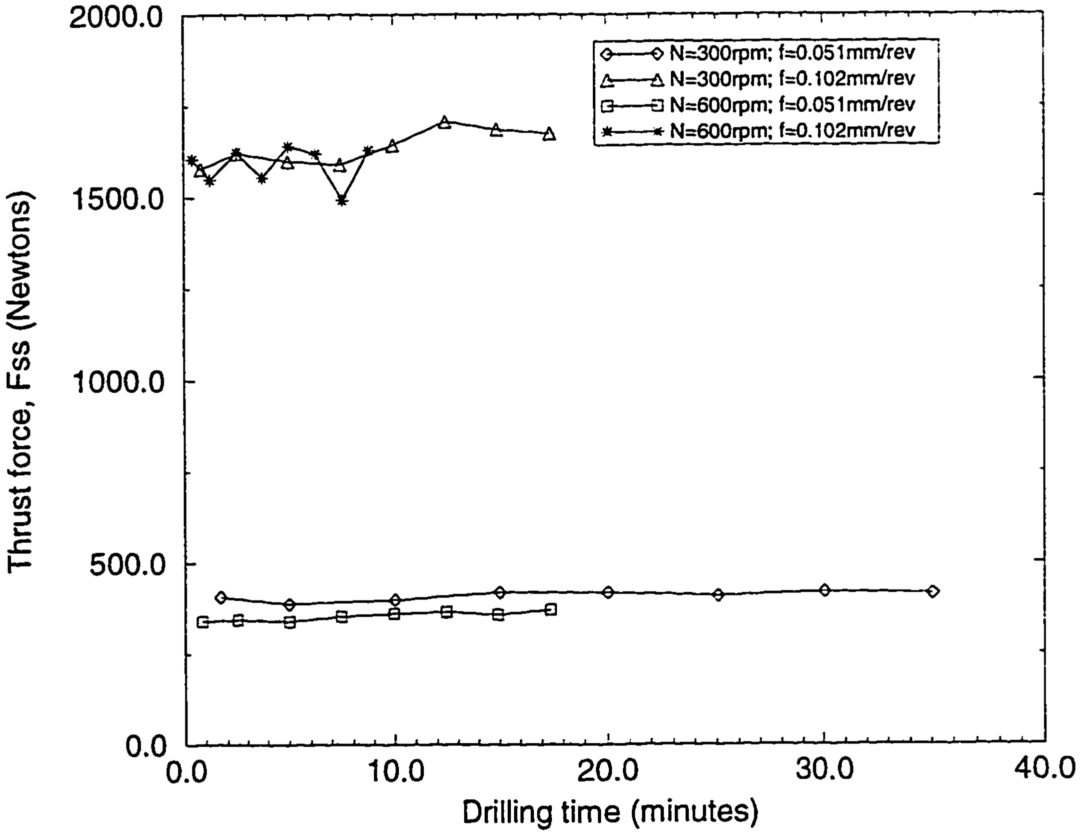

Figure 4.2: Plot of Steady State Thrust Force for the Commercial Drills at Various Cutting Conditions

rate. which in turn increases the compressive forces exerted by the feed motion of the tool into the worpiece material [7].

The curves of the steady state torque(Tss) versus the machining time of holes drilled by the experimental drill are plotted in Figure 4.3 from the respective cutting conditions data of Table 4.7. The curves reveal a slight increase in the torque

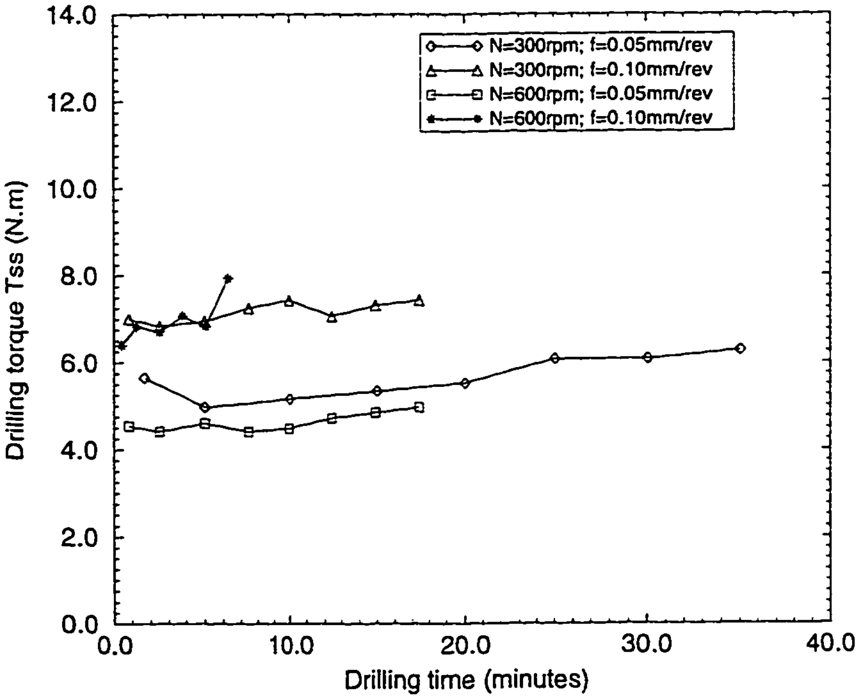

Figure 4.3: Plot of Steady State Torque for the Experimental Drills at Various Cutting Conditions

between the first hole and the twenty-first hole for the given sets of cutting conditions. The figure shows that when drilling at a given value of machining time and a certain value of speed the value of the torque for the higher level of feed rate(0.10 mm/rev) is higher than the values corresponding to the lower level of feed rate(0.05 mm/rev). On the other hand the torque curves corresponding to 600 rpm fall below those corresponding to the 300 rpm where drilling is performed at a feed rate of 0.05 mm/rev. At the feed rate of 0.10 mm/rev the torque curves corresponding to 300 rpm and 600 rpm cutting speeds appear to be at approximately the same levels.

Figure 4.4 shows the curves of the steady state torque(Tss) versus the number of holes drilled by the commercial drill plotted from the respective cutting conditions data of Table 4.8. Except for the curve corresponding to the speed of 600 rpm and feed rate of 0.10 mm/rev, the other curves are falling very near to each other. The torque values of the former curve is about twice those of the other three curves. The effect of increasing the feed still remains the same as observed for the experimental drill, i.e. the torque increases when the feed is increased. However, there seems to be relatively strong interaction between the cutting speed and the feed rate, which tends to cause the torque curves to cluster together at three cutting conditions. It is only at the extreme condition of high speed and high feed that there is a marked variation from this trend.

4.4 Effect of Machining Time on Surface Roughness

The average and the standard deviation of the drilled hole surface roughness values 'R_a' was computed for the three readings described in section 3.2.4 for each test

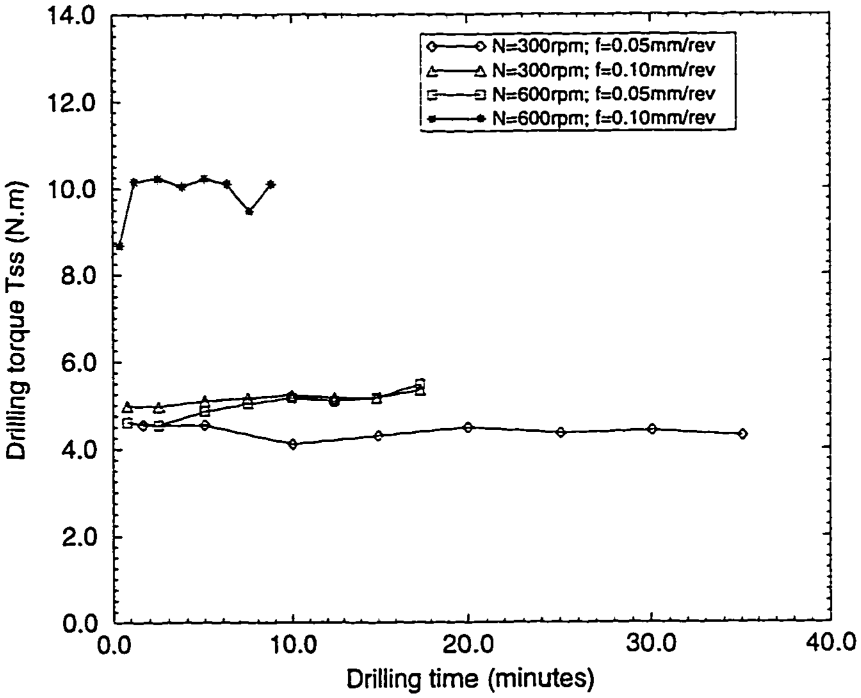

Figure 4.4: Plot of Steady State Torque for the Commercial Drills at Various Cutting Conditions

condition. The results are given in Table 4.9 and Table 4.10 for the experimental and commercial coated drills respectively. The drill used at the cutting condition of 600 rpm and 0.10 mm/rev, failed catastrophically at the beginning of the 16th hole. Possible reasons of premature drill failure could be attributed to clogging by the chips or to the drill misalignment in the chuck.

The center line average of surface roughness 'R_a' of the drilled holes has been plotted against the drilling time in Figure 4.5 for the experimental drills, and in Figure 4.6 for the commercial drills. A general conclusion which is immediately evident from these plots is that the surface roughness of a drilled hole deteriorates with increasing machining time. This is attributed to the progressive wear of the cutting tool as it continues to drill more holes. On the otherhand the effect of cutting speed is that, as the speed increases the hole surface roughness deteriorates for both experimental and commercial drills, as shown in Figures 4.5 and 4.6 at both levels of the feed rate. This may be attributed to the possible occurance of built-up-edge in the selected range of cutting speeds. This will lead to deterioration of the surface finish. It also evident from these figures that at both the levels of the cutting speeds an increase in the feed rate from 0.05 mm/rev to 0.10 mm/rev tends to increase the average surface roughness value R_a of the drilled holes for experimental as well as the commercial drills. In general, the hole surface roughness produced by the experimental drills are relatively lower compared to the surface roughness values of the holes produced by the commercial drills.

4.5 Effect of Machining Time on Tool Wear

The tool wear data obtained using the optical measurement procedure described

Table 4.9: The Average "Ave." and Std. Deviation "SD" of the Center Line Average (R_a) of the Drilled Hole Surface Roughness for the Experimental Drills

Drilled Hole Surface Finish Data $R_a(\mu m)$								
	300 rpm, 0.05mpr		600 rpm, 0.05mpr		300 rpm,0.10mpr		600 rpm, 0.10mpr	
Hole	Ave.	SD	Ave.	SD	Ave.	SD	AV	SD
1	6.230	0.512	4.300	0.036	5.660	0.217	5.640	0.070
2	4.580	0.569	3.590	0.606	5.200	0.710	5.027	0.603
3	4.350	0.554	3.830	0.581	5.627	0.630	5.303	0.610
4	4.497	0.525	4.380	0.600	5.903	0.549	5.123	0.557
5	4.600	0.556	4.293	0.551	5.640	0.572	5.727	0.681
6	5.093	0.555	4.450	0.572	6.133	0.567	5.277	0.595
7	4.890	0.524	4.603	0.622	6.490	0.567	6.020	0.512
8	5.340	0.514	4.903	0.587	6.757	0.629	5.667	0.508
9	5.310	0.560	4.773	0.578	6.583	0.557	6.427	0.534
10	5.583	0.534	5.543	0.595	7.133	0.626	7.790	0.546
11	6.117	0.527	4.937	0.575	7.583	0.644	8.467	0.482
12	6.550	0.546	5.750	0.563	7.777	0.690	7.547	0.659
13	6.350	0.552	6.150	0.589	8.303	0.618	9.907	0.628
14	6.923	0.530	6.443	0.560	8.877	0.638	10.727	0.497
15	7.350	0.534	7.417	0.479	8.567	0.558	10.027	0.405
16	7.653	0.546	7.327	0.628	9.260	0.580	*	
17	7.840	0.682	7.730	0.590	9.683	0.567		
18	8.520	0.501	8.267	0.542	10.223	0.609		
19	8.867	0.535	8.313	0.538	10.420	0.687		
20	8.783	0.544	8.840	0.598	10.433	0.497		
21	8.850	0.509	8.653	0.552	10.557	0.499		
* - premature drill failure, mpr = mm/rev. Drilling time is calculated by Eqn-4.6								

Table 4.10: The Average "Ave." and Std. Deviation "SD" of the Center Line Average R_a of the Drilled Hole Surface Roughness for the Commercial Drills

Drilled Hole Surface Finish Data $R_a(\mu m)$								
	300 rpm, 0.05mpr		600 rpm, 0.05mpr		300 rpm, 0.10mpr		600 rpm, 0.10mpr	
Hole	Ave.	SD	Ave.	SD	Ave.	SD	AV	SD
1	6.050	0.226	5.020	0.203	6.520	0.010	6.530	0.743
2	6.147	0.234	5.597	0.623	6.803	1.259	6.350	0.066
3	6.367	0.406	5.177	1.079	6.663	0.517	6.290	0.090
4	6.707	0.545	5.637	0.811	7.863	1.223	6.540	0.383
5	7.507	0.335	6.607	0.806	7.503	0.656	7.090	0.263
6	7.997	1.367	7.197	0.552	8.143	0.465	7.970	0.151
7	8.707	0.306	7.313	0.777	9.963	1.006	9.070	0.201
8	9.117	0.355	8.543	0.690	9.783	0.534	9.290	0.066
9	9.797	0.479	8.340	0.135	10.453	0.594	9.660	0.144
10	9.237	1.000	8.540	0.607	10.283	0.555	10.350	0.030
11	9.607	0.800	8.157	0.350	10.583	0.531	10.020	0.181
12	9.607	2.120	8.733	1.157	11.013	1.113	10.110	0.190
13	9.917	0.345	8.553	0.588	10.773	0.524	10.000	0.191
14	10.537	0.471	9.253	0.902	12.133	0.343	10.010	0.282
15	11.217	0.311	10.143	0.771	12.133	0.517	11.360	0.195
16	11.087	0.439	9.723	1.960	11.563	0.457	10.920	0.314
17	11.567	0.604	9.833	1.123	12.163	0.280	12.030	0.225
18	12.327	0.240	11.593	0.676	12.863	0.222	12.320	0.449
19	12.767	0.751	11.823	0.510	12.943	0.782	12.510	0.330
20	12.887	0.273	12.077	0.442	13.363	0.529	13.010	0.193
21	12.827	0.311	12.060	0.446	13.387	0.592	13.020	0.020
Drilling time is calculated by Eqn-4.6, mpr = mm/rev.								

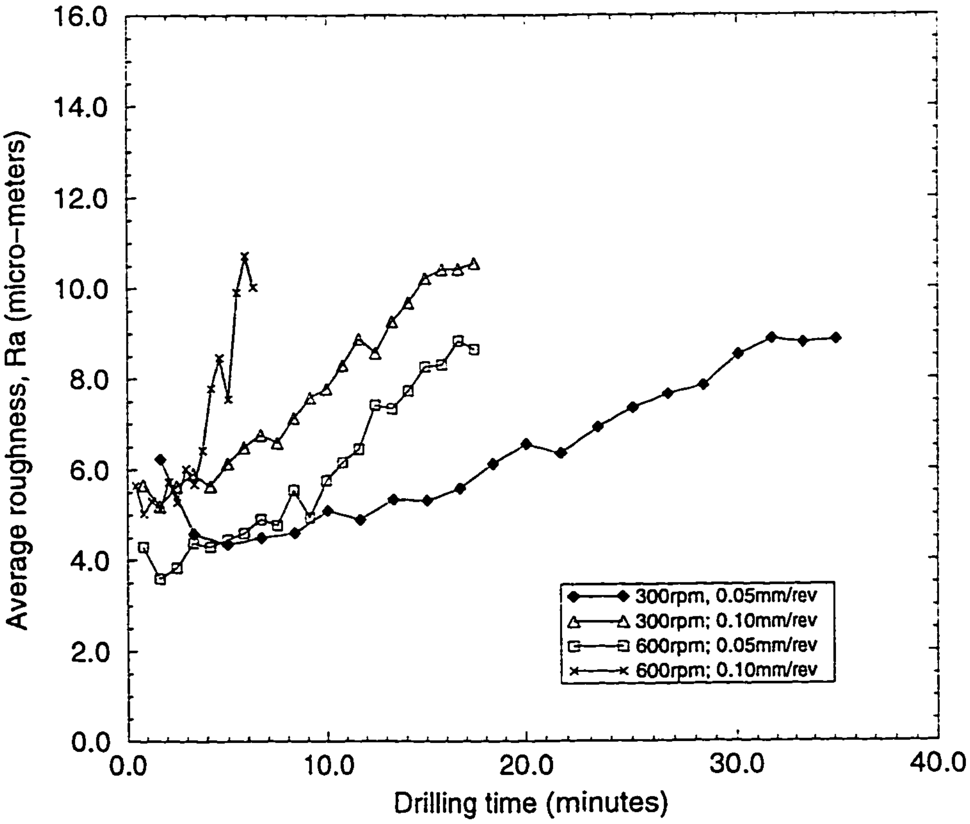

Figure 4.5: Surface Roughness Vs. Drilling Time for Experimental Drills

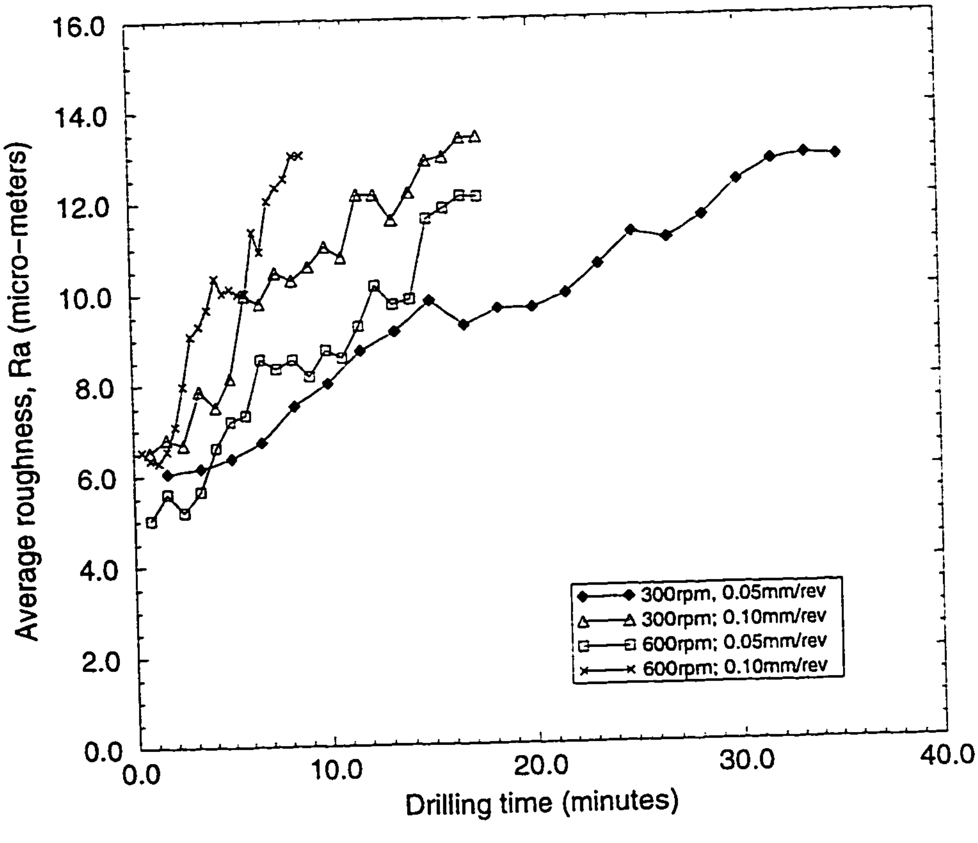

Figure 4.6: Surface Roughness Vs. Drilling Time for Commercial Drills

Table 4.11: Flank Wear Data at Locations A.B and C(Figure 3.6) of Experimental Drills

Speed 300 rpm. Feed 0.05 mm/rev				
Hole	Time(min)	A	B	C
3	5.00	0.25	0.09	0.05
6	10.02	0.26	0.09	0.05
9	15.03	0.28	0.09	0.05
12	20.04	0.29	0.10	0.06
15	25.05	0.31	0.11	0.06
18	30.06	0.32	0.11	0.07
21	35.07	0.33	0.11	0.07
Speed 600 rpm. Feed 0.05 mm/rev				
3	2.50	0.30	0.10	0.06
6	5.00	0.34	0.12	0.07
9	7.47	0.36	0.12	0.07
12	9.96	0.39	0.12	0.07
15	12.45	0.42	0.14	0.08
18	14.94	0.44	0.15	0.09
21	17.43	0.46	0.1505	0.10
Speed 300 rpm, Feed 0.10 mm/rev				
3	2.50	0.27	0.09	0.06
6	5.00	0.32	0.10	0.07
9	7.47	0.34	0.12	0.08
12	9.96	0.36	0.12	0.08
15	12.45	0.40	0.14	0.08
18	14.94	0.42	0.14	0.08
21	17.43	0.43	0.15	0.09
Speed 600 rpm. Feed 0.10 mm/rev				
3	1.25	0.39	0.14	0.09
6	2.50	0.47	0.16	0.10
9	3.78	0.50	0.17	0.11
12	5.04	0.52	0.18	0.11
15	6.30	0.55	0.19	0.12

Table 4.12: Flank Wear Data at Locations A,B and C (Figure 3.6) of Commercial Drills

Speed 300 rpm, Feed 0.05 mm/rev				
Hole	Time(min)	A	B	C
3	5.00	0.25	0.08	0.05
6	10.02	0.29	0.10	0.06
9	15.03	0.31	0.11	0.06
12	20.04	0.33	0.11	0.07
15	25.05	0.34	0.12	0.07
18	30.06	0.35	0.12	0.07
21	35.07	0.36	0.12	0.08
Speed 600 rpm, Feed 0.05 mm/rev				
3	2.5	0.34	0.11	0.07
6	5.00	0.38	0.13	0.08
9	7.47	0.39	0.13	0.08
12	9.96	0.41	0.13	0.08
15	12.45	0.45	0.15	0.09
18	14.94	0.50	0.17	0.10
21	17.43	0.51	0.17	0.10
Speed 300 rpm, Feed 0.10 mm/rev				
3	2.50	0.30	0.10	0.06
6	5.00	0.33	0.11	0.07
9	7.47	0.35	0.12	0.07
12	9.96	0.37	0.13	0.07
15	12.45	0.41	0.14	0.08
18	14.94	0.43	0.14	0.09
21	17.43	0.44	0.15	0.09
Speed 600 rpm, Feed 0.10 mm/rev				
3	1.25	0.45	0.15	0.09
6	2.50	0.51	0.17	0.10
9	3.78	0.54	0.18	0.11
12	5.04	0.56	0.19	0.11
15	6.30	0.59	0.20	0.12
18	7.56	0.62	0.21	0.12
21	8.82	0.65	0.21	0.13

in section 3.2.2 for the experimental and commercial drills are shown in Tables 4.11 and 4.12 respectively. From Table 4.11, the maximum wear of the drill flank corresponding to the outer point of the cutting edge(point A), in Figure 3.6, is plotted against the drilling time at the different cutting speeds and feeds, to obtain the curves shown in Figure 4.7 for the experimental drills. The wear curves at the respective speeds and feed rates appear to have a linear relationship with the machining time, as indicated by the fitted solid lines, i.e. they represent the steady wear rate region [35] of the drill flank. It can be seen from these curves that increasing the cutting speed from 5.99 m/min (300 rpm) to 10.97 m/min(600 rpm) results in increased wear. The effect of feed rate is also similar to that of cutting speed i.e. the amount of flank wear increases with the increase of feed rate. The tool wear curves of the commercial drills plotted from the data of Table 4.12 shown in Figure4.8 are similar to those of the experimental drills in Figure 4.7.

The tool life constants in the Taylor's tool life equation $VT^n = C$ were determined from the tool life curves for both the experimental drill and the commercial drill. The variables V and T are the linear cutting speed and tool life respectively and n and C are constants. The values of these constants are calculated from tool life data obtained from tool wear curves (using wear criteria of VB = 0.34mm) in Figure 4.7 and Figure 4.8 for the experimental drills and commercial drills respectively. It is reported by Tipnis and Christopher [36] that the normally used wear criteria for drill life testing in industry is VB=0.38mm for HSS and Carbide tools, in this case VB=0.34mm was chosen to avoid errors associated with extrapolation in the region beyond the range of the experimental cutting conditions. The tool

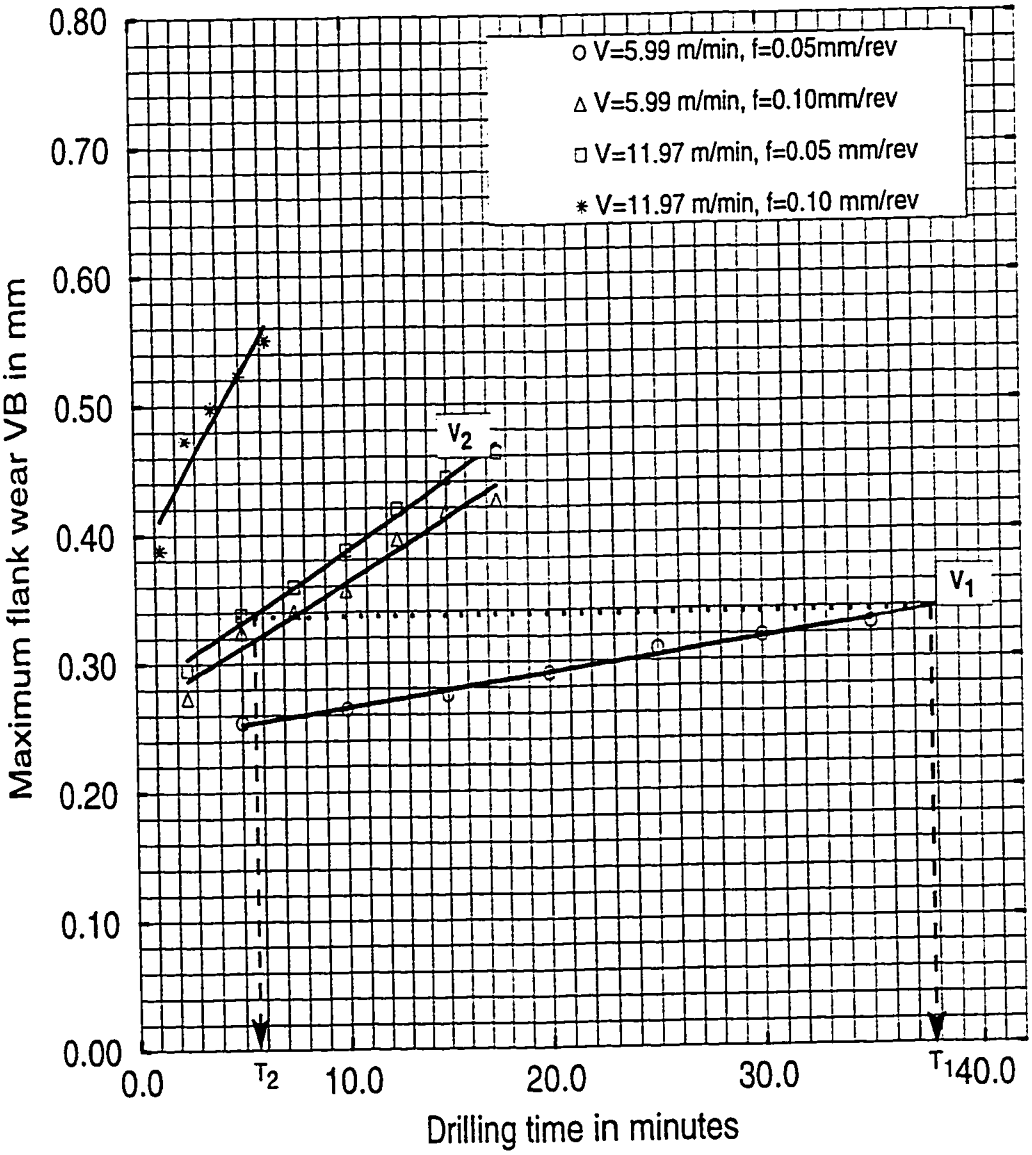

Figure 4.7: Flank Wear Vs. Machining Time for the Experimental Drills

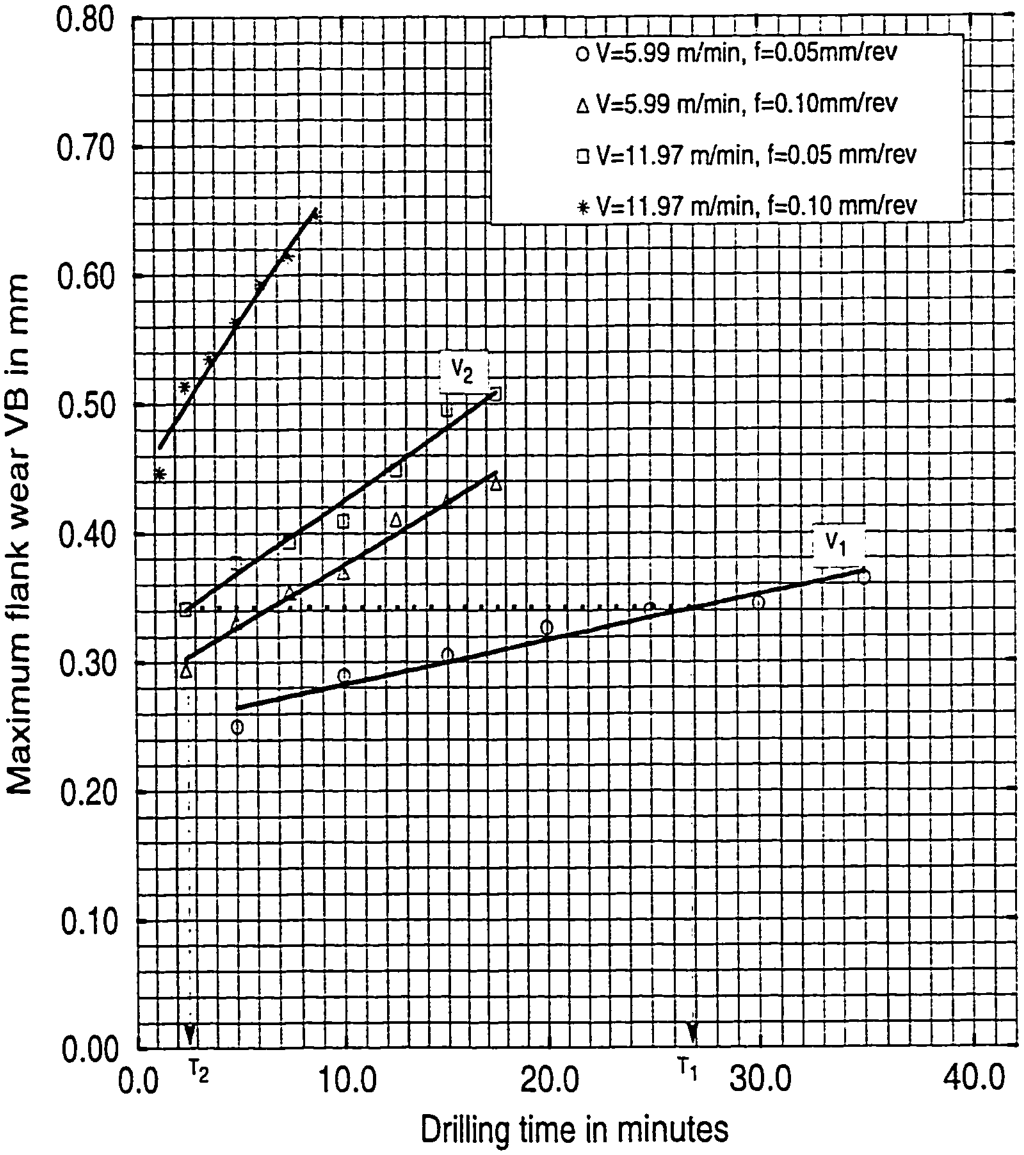

Figure 4.8: Flank Wear Vs. Machining Time for the Commercial Drills

Table 4.13: Values of Tool Life Constants 'n' and 'C' for Experimental and Commercial Drills

Drill Type	Cutting Conditions		Tool Life Constants	
	Speed(m/min)	Drilling time(min)	n	C
Experimental Drill	5.99 11.97	38 5.8	0.37	22.85
Commercial Drill	5.99 11.97	26.9 2.5	0.29	15.66

life is defined as the time in minutes it takes to reach the specific wear criterion under specified process conditions [37]. The calculated tool life constants 'n' and 'C' are given in Table 4.13. The values of the constant 'n' which is a characteristic of the tool material was obtained as 0.37 for the experimental drills and 0.29 for the commercial drills respectively. Typical values of n, as reported in literature [37] is 0.1 for HSS, 0.25 for cemented carbides, 0.30 for coated carbides and 0.40 for ceramic tools. Since n is a characteristic of the tool material, the values of n for the experimental and commercial drill show that these drills have a life similar to coated carbide tools, but its life should be less than ceramic tools. Both the commercial and the experimental drills showed 'n' values greater than for uncoated HSS and uncoated cemented carbide cutting tools. The value of n and C for the experimental drills are relatively higher compared to the values of n and C for the commercial drills. This indicates that experimental drills have higher tool lives compared to the commercial drills.

4.6 Evaluation of Drill Wear by Micro-PIXE

This section describes the evaluation of the drill wear patterns which were generated by micro-PIXE technique as described in section 3.2.3. Distribution maps of the workpiece and tool material trace elements are used to determine the wear regions of the drill bits. Nickel was used as an indicator for workpiece material because of its much higher concentration in the workpiece material as compared to the tool base material. Titanium was used as a monitor for the tool coating.

As the measured elemental distribution maps were limited to a size of 540×540 μm^2, two maps were used to cover the area of interest on the flank face edge and 4 to 6 maps were used for the chisel edges. In all these maps the dark region corresponds to higher concentration and light region corresponds to lower concentration of the trace elements. The composition of tool base material and workpiece material obtained partly from PIXE analysis, is given in Table 4.6. For elements having energy levels below 5 KeV such as Si, S, P etc., PIXE values cannot be used without accurate calibration of the detector(see section 3.2.3). Therefore typical values corresponding to nominal compositions were obtained from literature [38].

4.6.1 Analysis of Wear Patterns on the Flank Faces of the Experimental and Commercial Drills

Figurs 4.9, shows the elemental distribution maps of Ti, Fe, Ni and Mo for the experimental and commercial drills near the outer corner of the flank faces. As seen from Table 4.6, Ti is present in the drill coating, Ni is available in abundance in the workpiece material and in trace amounts in the tool base material, Fe and Mo are

Table 4.14: Constituents of the Tool Base Material from PIXE Analysis.
(Values obtained from literature are shown in brackets)

Element	C	Si	V	Cr	Mn	Co	Ni	Mo	W	P	S	Fe(bal)
Expt. Drill	(1.05)	(0.55)	1.80	4.10	0.37	1.00	(0.30)	(9.20)	(2.10)	-	-	79.53
Comm. Drill	(1.05)	(0.55)	1.80	3.70	0.30	0.80	(0.30)	(9.20)	(2.10)	-	-	80.2
work mat.	(0.15)	(1.0)	-	17.60	1.78	0.65	8.48	0.37	-	(0.20)	(0.15)	69.77

available in comparable proportions in both tool and workpiece materials. From the Fe maps shown in Figure 4.9(a) and Figure 4.9(b), three regions can be distinguished near the cutting edge: In region I, Fe from the tool base material is attenuated from the TiN coat, there is no workpiece material in this region. In region II. the TiN layer is worn out. There is no work material deposition therefore high Fe yield is seen from the exposed tool base. In region III, TiN coat is worn out, but there is also adhesion of work piece material on the exposed tool base. Therefore low Fe yield is observed in this region. The elemental composition and wear patterns in each of these regions are discussed below:

- Region I(TiN coat):

  For the experimental drill the Ti yeild shown in Figure 4.9(c) is getting lower towards the boundary of the coat which does not appear as a smooth line. The thinning of the coat near the boundary is an indication of gradual wear as a result of the machining process. In contrast to the experimental drill, the Ti map(figure 4.9(d)) for the commercial drill shows a uniform Ti yeild all over and up to the very edge of the coat, which appears as a sharp and smooth line. This observation indicates that the coat has fractured and spalled off from the tool. The observed differences in distribution maps of TiN coats of the experimental and commercial drills leads to the proposition that the TiN coat of the experimental drill is removed by abrasive wear whereas the TiN coat of the commercial drill is removed by fracture and spalling. The abrasive wear of the experimental drill coat is generally unexpected, because TiN is a ceramic material having higher hardness than the work piece material, and is normally expected to be removed by flaking. The observed abrasive wear

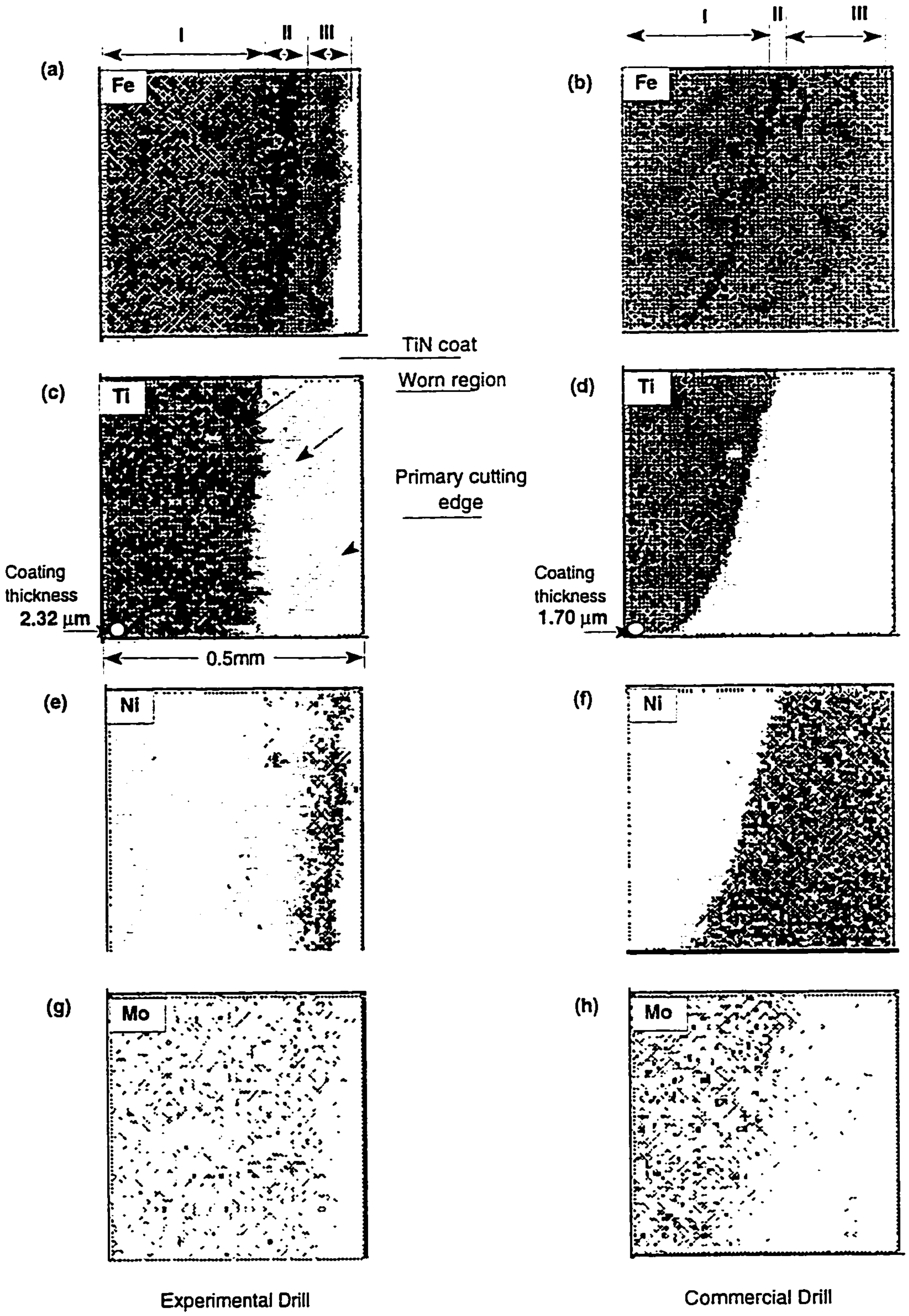

Figure 4.9: Elemental Distribution Maps of Ti, Fe, Ni and Mo on the Flank Face of Experimental and Commercial Drills

of the TiN coat is only possible if the coating is strongly bonded to the tool base. It appears that the intermediate nitride layer of the experimental drill provided the high adhesive strength between the TiN coat and the tool base. Dislodged particles from the TiN coat itself of the experimental drill may act as abrasive grains. In the case of commercial drill, which lost its TiN coating through fracture and spalling, no evidence of any intermediate nitrided layer was observed.

- Region II(High Fe yield region):
  The boundaries of region II are defined by those of Fe maps(figure 4.9(a) and 4.9(b)). Lack of Ni yield in Figure 4.9(e) for the experimental drill indicates absence of workpiece material. The high yield of Fe in region II as indicated by Figure 4.9(a) as compared to the attenuated Fe below TiN coat in region I indicates an exposed tool base material. The lack of work material on region II as evidenced by the lack of Ni yield is explained by the effect of the hard plasma nitrided layer between the tool base and the TiN coat which acts as a solid lubricant and prevents the sticking of the work material to the worn tool in this region [39]. In the case of the commercial drill the sharp edge of the spalled coating at the boundary of the worn region and the TiN coat acts as a step and prevents the workpiece material from sticking to the tool base in the very vicinity of the coat. It seems that the mechanisms leading to an openly exposed tool base material(region II) for the commercial and experimental drills are different. So far we have no evidence of any pretreatment prior to the TiN coating of the commercial drill as compared to the experimental drill.

- Region III(Sticking Workpiece Material):
  The boundaries of region III are defined by those of the Ni maps shown in Figure 4.9(e) and Figure 4.9(f) for the experimental and commercial drill respectively. The concentration of the sticking workpiece material(Ni) appear to be high at the very cutting edge for both the drills. The presence of relatively high Ni yield in this region for both types of drills indicates the presence of an adhered layer of work material. The presence of an adhered layer of work material in region III, of the experimental drill, contrary to its absence in region II, indicates that the thin plasma nitrided layer was lost from region III and the tool base material was exposed. This caused the work material to adhere to the tool base material in this region. The relatively high yield of Ni in region III of the commercial drill shown in Figure 4.9(f) indicates uniform adhesion of work material on the worn region of the tool base material.

- The elemental maps in regions II and III of the experimental drill leads to the conclusion that wear on the flank face results in the "cutting" of the nitrided layer at a shallow angle which leads to reduced thickness of the TiN coat in region I, exposed plasma nitrided layer in region II and completely exposed tool base material with work material adhesion in region III. These regions are shown schematically for the experimental drill in Figure 4.10(a). This is confirmed by the inability of the work material to stick to the TiN coat of the experimental drill in region I and the nitrided layer in region II as indicated by Ni map in Figure 4.9(e). On the other hand, Figure 10(b) shows the proposed mechanism of wear for the commercial drill which leads to the adhesion of work material to the worn tool base and the absence of work piece material at the foot of the spalled TiN coat and also on TiN coat. Wear of the commercial drill appears to result from the fracture and spalling of the hard and brittle TiN coat as discussed above.

- Not fully understood result for the commercial drill is the elemental distribution map for Mo shown in Figure 4.9(h). Molybdenum, is an alloying element with high concentration in the tool material, shows higher yield at the TiN coat(region I) as compared to the region of sticking work material(region III). From a hole in the coat shown in the Ti map and a corresponding higher yield in the map at 2.3 KeV(S-K_α and Mo-L lines), we conclude that the coat itself does not contain Mo under the assumption that the coat composition is uniform. The W-M line distribution map at 1.78 KeV which originated from tungsten in the tool base, shows similar yield in region I and region III. This means, the thickness of the sticking work material is similar to TiN layer thickness. These observations cannot explain the Mo yield distribution map. There could exist a Mo rich layer between tool base and coat. This would be an indication for a pretreatment of the commercial drill prior to the coating process.

4.6.2 Analysis of Wear Patterns on the Chisel Edges of the Experimental and Commercial Drills

Figure 4.11 shows the elemental distribution maps of Ti and Ni on the chisel edge of the experimental and commercial drills. For the experimental drill the chisel edge itself is intact as was also observed from the secondary electron map. The face of

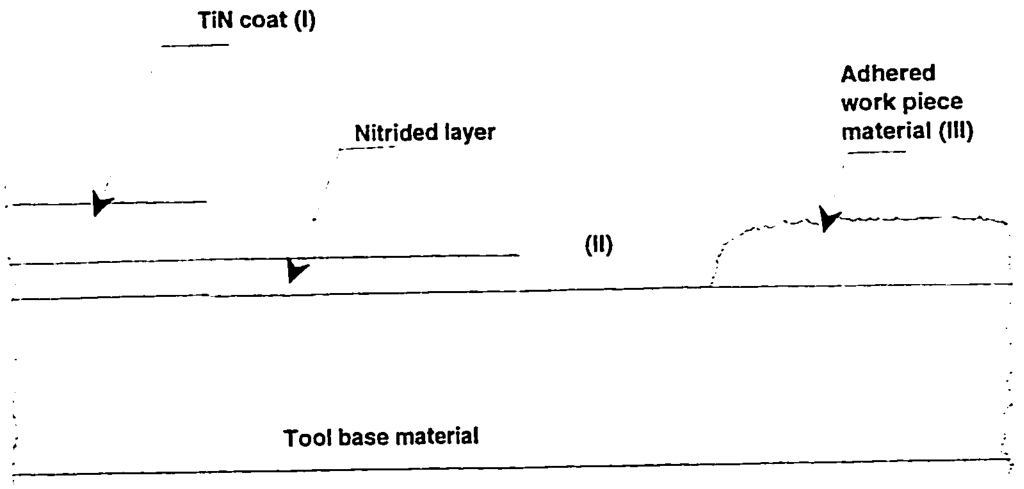

(a) Experimental Drill

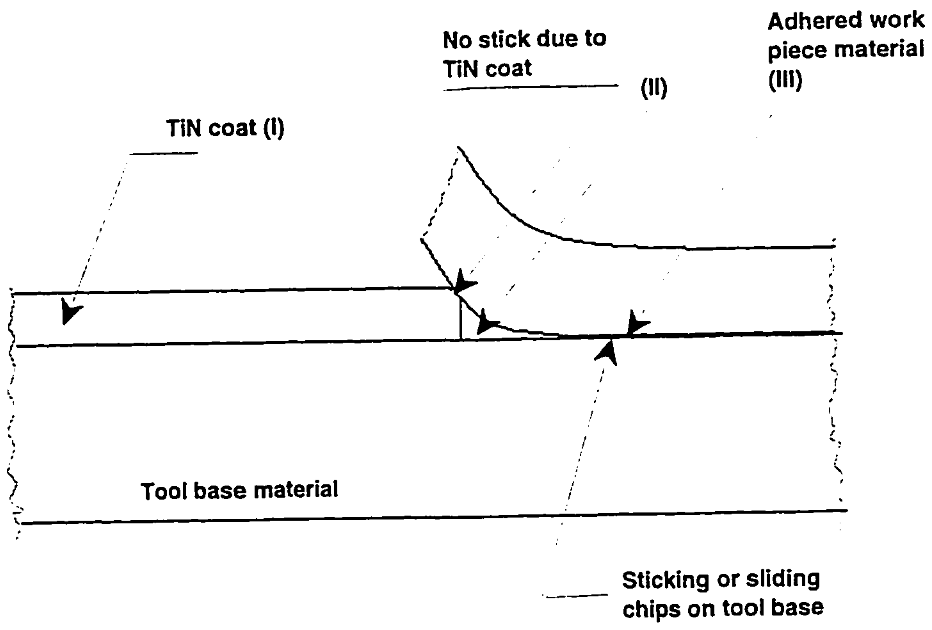

(b) Commercial Drill

Figure 4.10: Schematic Representation of the Observed Wear Regions on the Flank Face of (a)Experimental Drill and (b) Commercial Drill

the chisel edge shows a wear pattern similar to that of the flank face with a region of sticking work material immediately followed by the TiN coat with no freely exposed tool in between. Near the center of the chisel edge the picture changes, and work material is found sticking all around the chisel edge. Wear scratches are clearly visible on the coat. Near the smooth boundary of the coat it appears that a well defined area is present with a reduced coating thickness. The worn region on the face of the chisel edge shows a triangular shape with the completely removed coat, a smooth boundary and no sticking work material. Beyond this worn area some work material appears to stick even on the coat.

For the commercial drill the chisel edge is completely worn out and is not clearly visible in the secondary electron map. Sticking work material is concentrated near the cutting edge and a few dots are scattered over the triangular shaped worn area below the location of the original chisel edge. Interestingly, there is an appearance of Mn correlated with S, indicating the possibility of the formation of MnS near the center of the chisel edge. The coat also seems to have flaked off leaving a very rough boundary.

Differences in wear pattern between the chisel edge and flank face is attributed to the nature of the interaction between the workpiece and the tool at the two locations. On the flank face machined chips flow on it, whereas deformation and extrusion processes occur at the chisel edge.

4.6.3 Coating Thickness

As the proton beam penetrates the TiN coat it is possible to determine the coating thickness as explained in Chapter 3. The locations on the flank face and the face

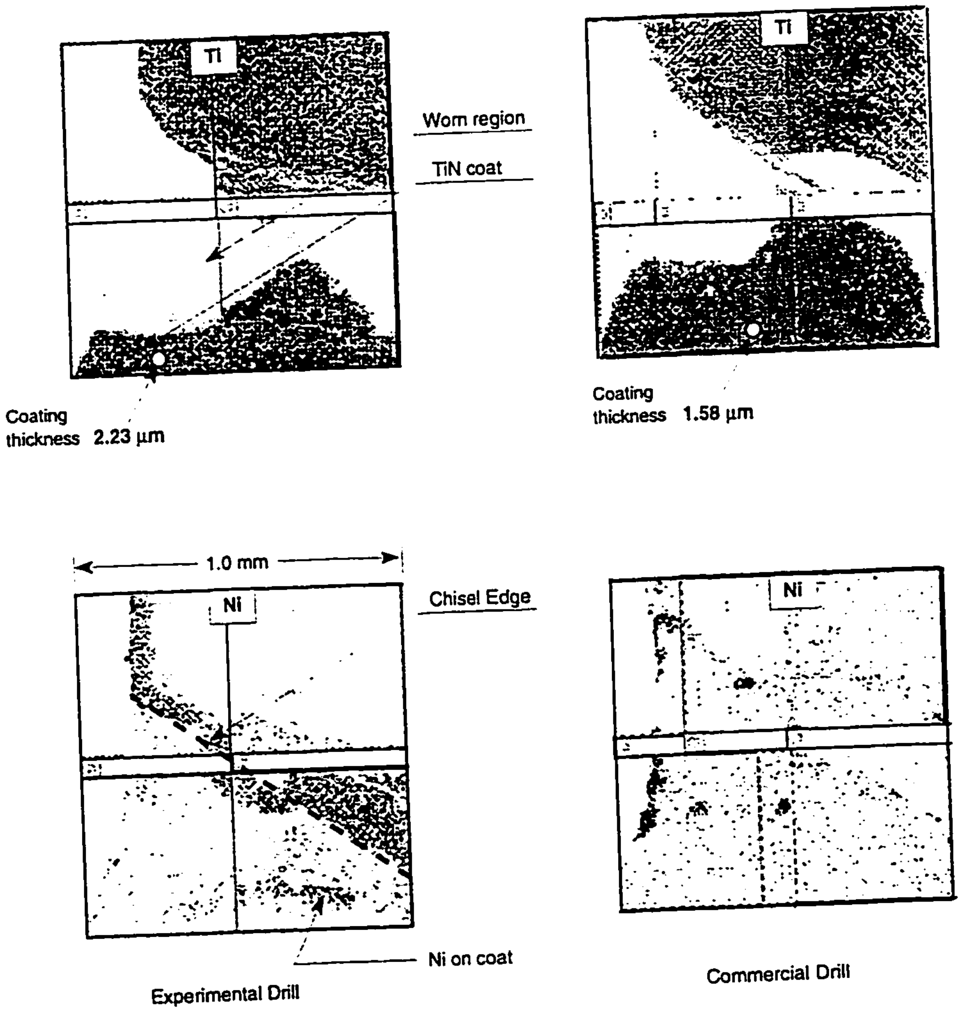

Figure 4.11: Elemental Distribution Maps of Ti and Ni on the Chisel Edges of Experimental and Commercial Drills

of the chisel edge, where these coating thicknesses were determined are shown by a white dot in the Ti distribution maps for both the experimental and the commercial drills. The original thicknesses were determined on the shank of the drill and on the flank face away from the cutting edge to ensure that the coating thickness has not been affected by wear. For the commercial drill all locations show values of about 1.6μm, indicating a uniform coating thickness. For the experimental drill the thickness of the coat was measured 3.2μm on the shank and approximately 2μm on the flank face and the chisel edge region. The observed variations in the coating thicknesses are attributed to the quality of the coat.

Chapter 5

EVALUATION OF THE RELATIVE PERFORMANCE OF THE TWO TYPES OF TWIST DRILLS

The purpose of the present study was to evaluate and compare the performance of the experimental TiN coated drill bits with the performance of the conventional commercial TiN coated drills. The performance evaluation variables are the drilling thrust force, cutting torque, flank wear, and the drilled hole surface roughness and the flank wear patterns. In chapter-4 the performance variables of both types of drills have been presented in tabular and graphical form. A quantitative comparison of the relative performance of the two types of drill bits was not included. In this chapter the experimental results are evaluated quantitatively and compared by using statistical techniques.

Paired data sets of the performance evaluation variables corresponding to the experimental and commercial TiN coated twist drills are constructed from the data of the series of holes drilled to study the effect of machining time on the performance variables. Two nonparametric paired sample tests together with Kolmogorov-Smirinov test are used to statistically evaluate the relative performance of the two types of TiN coated twist drills.

5.1 The Statistical Testing Methods

5.1.1 Matched Pair Testing

The underlying principles of a matched paired experiment is that each sample unit in the experimental group is matched to its counterpart in the control group [40] Each resulting pair is then evaluated as a single entity. The objective of matching is to obtain units in each pair which are alike in most of the factors that might contribute to the level of variable being considered. Therefore any differences in the pairs can then be explained on the basis of differences in treatments rather than by other causes. For example the drilling thrust force values for drilling a set of holes by experimental drill bits are compared with the thrust force values corresponding to a similar set of holes drilled by the commercial drills at identical cutting conditions. A point to be noticed here is that getting an ideally matched pair is not always possible in experimentation [40], hence near ideal pairs are used.

5.1.2 Kolmogorov-Smironov Test

The Kolmogorov-Smironov(K-S) test is a test for comparing the distributions of two samples, i.e., it determines whether two distribution functions associated with two populations are identical. The K-S test is based on calculating the maximum vertical distance between the cumulative distribution functions of the two samples. If this distribution is large enough, the P-value will be small; where P is the probability of accepting the null hypothesis. The assumption of the null hypothesis is that the difference between the two distributions being compared is not statistically significant at the 95% confidence level.i.e.:

Ho: $F(x_i) = G(y_i)$

where: $F(x_i)$ is the cumulative distribution function of x_i, where x_i corresponds to the values of the first data set in the pair.

and $G(y_i)$ is the cumulative distribution function of y_i, where y_i corresponds to the values of the second data set in the pair

A P-value less than 0.05 indicates that the null hypothesis should be rejected.

5.1.3 Sign Test and Wilcoxon's Signed Rank Test

Two non parametric paired sample tests were used in this study, namely the Sign test and the Wilcoxon's signed rank test[40]. The sign test is used for testing whether one random variable in a pair(x,y) tends to be larger than the other random variable in the pair. This test is concerned only with the sign of the paired differences and not their relative sizes. The only requirement is that the data should be at least ordinal.

The Wilcoxon's signed rank test is a non parametric matched pair test. It is based on the difference between the observed values for each matched pair. It makes no stipulation regarding the nature of the population distribution. other than that they be identical. The test statistic for both these tests are the median values of the matched pairs.

5.2 Test Procedure

The Sign test and the Wilcoxon's Signed Rank test was implemented using the Statgraphics statistical package according to the sequence in the flow diagram shown in Figure 5.1. As can be seen from this figure the first step involves the comparison of the two data sets to determine whether they come from identical distributions, by using the Kolmogorov-Smirinov test. This was necessary to satisfy the assumptions of the Wilcoxon's signed rank test which requires that the two distributions be identical. The results of this K-S test determine which test will be used for hypothesis testing. If the distributions are not identical then the sign test will be used instead of the signed rank test. The following steps are performed during the Wilcoxons Signed Rank test or the Sign test; whichever was used .

Step 1: Testing equality of medians of the paired data sets

Null Hypothesis Ho: the location parameter(median) is the same for the two paired samples, i.e. $M(x_i) = M(y_i)$ for all i. This is tested against the alternate hypothesis

H1: $M(x_i) \neq M(y_i)$

where: $M(x_i)$ is the median of the data set pertaining to (x_i).

Where (x_i) is the ith element of the first data set and (y_i) is the corresponding

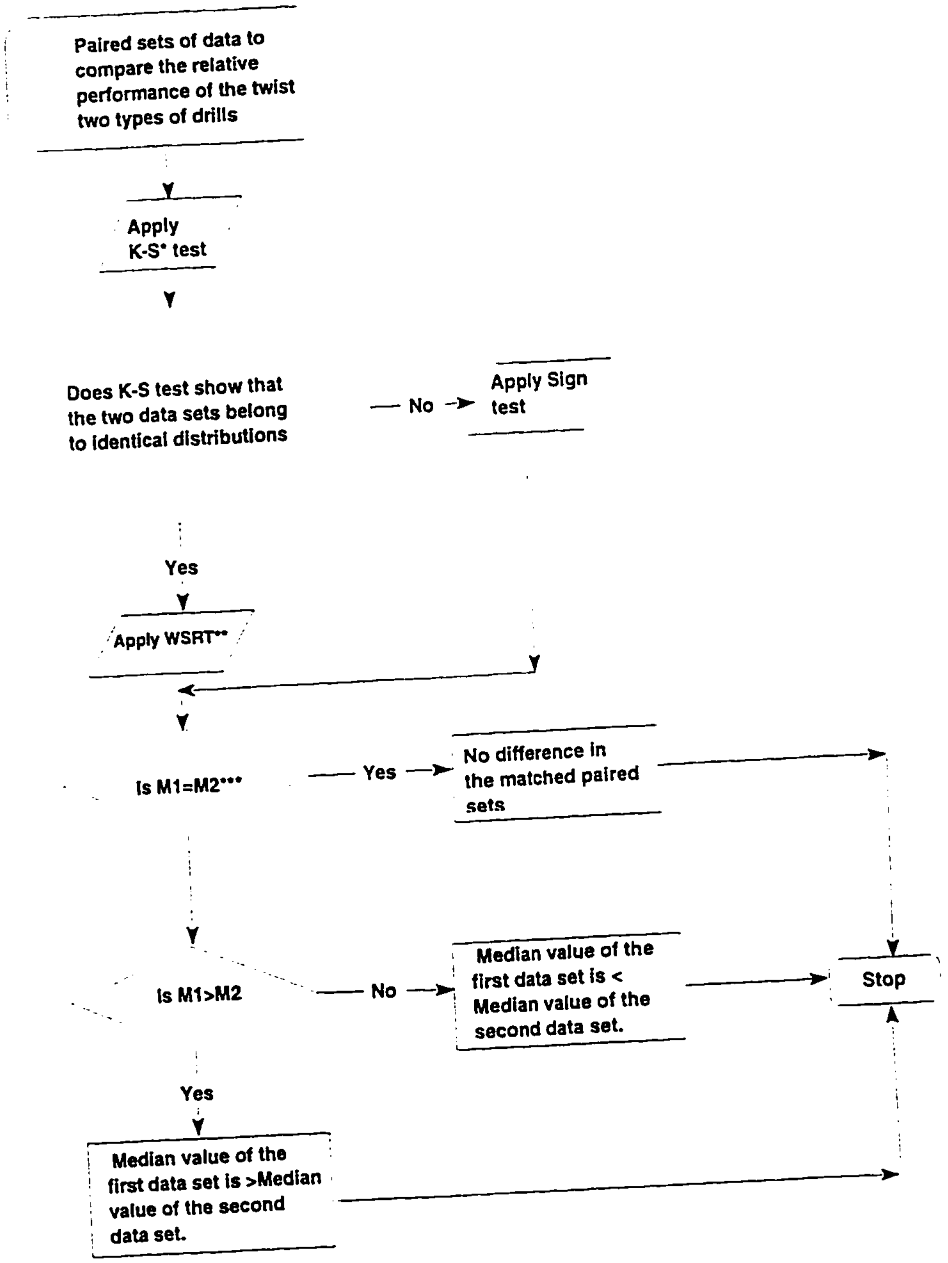

- K-S = Kolmogorov Smironov test

**WSRT= Wilcoxon's Signed Rank Test,

***M1= Median Value of 1st data set,
M2= Median Value of 2nd data set.

Figure 5.1: Flow Diagram for Statistical Testing and Comparison

ith element of the second data set. Similarly $M(y_i)$ is the median of the data set pertaining to (y_i),

Step 2: Testing whether the median of 1st data set is 'Greater Than', or 'Less Than' the median of the 2nd data set

In this case the null hypothesis may be considered to indicate whether the values x_i in the first set tend to be smaller than the values y_i in the second set.

Null hypothesis for this test is Ho: $M(x_i) < M(y_i)$ for all i. This is also tested against the alternate hypothesis:

H2: $M(x_i) > M(y_i)$ for all i

where $M(x_i), M(y_i)$, etc have the same definitions as in step-1.

5.2.1 Illustration of the Matched Pair Testing Method:

The first step is to prepare the paired data sets from the corresponding performance variables data of the experimental and the commercial drills performed at the same cutting conditions. To illustrate the procedure, the data set consisting of the thrust force values of the 1st, 3rd, 6th, 9th, 12th, 15th, 18th and 21st hole of the commercial drill from Table 4.6 are matched with the data set consisting of the thrust force values of the 1st, 3rd, 6th, 9th, 12th, 15th, 18th and 21st hole of the experimental drill from Table 4.5 to form the paired data sets shown in Table 5.2.1 at the same cutting condition of speed=300rpm and feed rate=0.05 mm/rev. In this table F_c = Steady state drilling thrust force for the commercial drill and F_e = Steady state drilling thrust force for the experimental drill respectively. The procedural steps given in

Table 5.1: Paired Data Sets for the Drilling Thrust Force

Hole No	F_c(N)	F_e(N)
1	406.02	427.58
3	387.15	411.41
6	397.93	432.97
9	419.49	459.92
12	416.80	459.92
15	408.71	462.61
18	419.49	468.00
21	414.10	500.34

Figure 5.1 is then followed. The Kolmogorov Smirinov (K-S) test was first used to check the null hypothesis Ho: that there is not a significant difference between the distributions of the two data sets.i.e. the two types of TiN coated drills are equal in performance. The P value(probability of accepting the null hypothesis) obtained from running this test on the statgraphics software was obtained as 0.00437. As the P-value is less than 0.05(which is 95% confidence interval) we reject the null hypothesis that the two distributions are identical and conclude that there is a statistically significant difference between the two distributions.

From the result of the K-S test, we know that the Wilcoxon's signed rank test cannot be used for further comparison of medians of these distributions. Therefore the Sign test is used. In this test the null hypothesis Ho is that the difference between medians is zero. This is tested against the alternate hypothesis that the difference between medians is not equal to zero. The null hypothesis is rejected if P-value is less than 0.05 at the 95% significance level.

On running this test on the Statgraphics software the P-value was obtained as 0.0133, therefore we reject the null hypothesis and conclude that the medians are not equal. Going a step further, we now test whether the median value of the steady state thrust force for the commercial drill is larger than the experimental drill. We reject this hypothesis at the 95% confidence level if the P-value is less than 0.05, and accept the alternate hypothesis that the median value of the thrust force for the commercial is smaller than the median value of the thrust force for the experimental drill. A P-value 0.0066 was obtained by conducting this test on the Statgraphics software. This result shows that the median value of the thrust force for the experimental drill(M_Fe) tends to be larger than the median value of the thrust force for the commercial drill(M_Fc)at this particular cutting condition. The above result is described in the first row of Table 5.3.

5.3 Relative Performance Evaluation of the Drills

5.3.1 The Drilling Thrust Force and Torque

Paired data sets of the steady state drilling thrust forces for the experimental and commercial drills at all cutting conditions are constructed and listed in Table 5.2. The procedure described in the foregoing example is used to compare the sets of the matched pairs of the steady state drilling thrust force at the given cutting conditions, the results of which are listed in Table 5.3. The median values of the drilling thrust force seems to be equal for both types of drills at three cutting conditions. The median value of the thrust force of the experimental drill is larger than that of the commercial drill at the cutting condition of speed=300rpm and feed rate=0.05mm/rev. The steady state torque data for the matched paired testing obtained from Table4.7 and Table4.8 is tabulated in Table 5.4. The matched paired

Table 5.2: Thrust Force Data for the Matched Pair Comparative Tests.

Hole no	N=300rpm f=0.05mm/rev		N=300rpm f=0.10mm/rev		N=600rpm f=0.05mm/rev		N=600rpm f=0.10mm/rev	
	F_c	F_e	F_c	F_e	F_c	F_e	F_c	F_e
1	406.02	427.58	1578.32	1470.52	338.65	330.56	1605.27	1308.82
3	387.15	411.41	1621.44	1564.84	344.04	338.65	1548.67	1376.20
6	397.93	432.97	1599.88	1578.32	338.65	333.26	1624.13	1443.57
9	419.49	459.92	1589.1	1713.06	352.12	344.04	1554.06	1481.3
12	416.8	459.92	1643.00	1847.81	360.21	349.43	1640.3	1454.35
15	408.71	462.61	1707.67	1847.81	365.60	352.12	1618.74	1556.76
18	419.49	468.00	1686.11	1928.66	357.51	360.21	1492.08	
21	414.10	500.34	1675.34	1928.66	370.98	373.68	1629.52	

F_c = Thrust force(Newtons) for commercial drill
F_e = Thrust force(Newtons) for experimental drill

Table 5.3: Results of Paired Comparison Tests for Thrust Force Data

Performance Variable: Fss = Steady State Drilling Thrust Force			
Speed (rpm)	Feed (mm/rev)	Test applied	Result
300	0.05	ST	$M_{F}e>M_{F}c$
600	0.05	WSRT	$M_{F}e= M_{F}c$
300	0.10	WSRT	$M_{F}e= M_{F}c$
600	0.10	ST	$M_{F}e=M_{F}c$
ST = Sign Test; SRT = Wilcoxon's Signed Rank Test			

testing was performed on these data sets at each of the given cutting conditions. The results of these tests are listed in Table 5.5. This table indicates that generally the median values of the torque seems to be smaller for the experimental drills compared with the commercial drills for all cutting conditions except at the cutting condition of speed=300rpm and feed rate=0.05mm/rev respectively, at which the median value of the torque for the value of the experimental drill tends to be greater than that of the commercial drill. This result is similar to the one obtained for the thrust force. A graphical representation of the matched pair testing for the drilling thrust force and the torque in the given ranges of cutting parameters is shown in Figure 5.2. The effect of the cutting conditions are easily seen from this performance grid. The median values of the steady state thrust force seems to be equal for both types of drills except at the lower value of speed and feed rate, in which case the experimental drill shows higher median values of the thrust force. The effect of feed rate on the median values of the torque of the two types of drills is that, the median

Table 5.4: Torque Data for the Matched Pair Comparative Tests.

Hole no	N=300rpm f=0.05mm/rev		N=300rpm f=0.10mm/rev		N=600rpm f=0.05mm/rev		N=600rpm f=0.10mm/rev	
	T_c	T_e	T_c	T_e	T_c	T_e	T_c	T_e
1	4.54	5.65	4.97	7.01	4.6	4.54	8.68	6.39
3	4.54	4.97	4.97	6.83	4.54	4.41	10.16	6.83
6	4.11	5.16	5.09	6.95	4.85	4.6	10.24	6.7
9	4.29	5.34	5.16	7.26	5.03	4.41	10.04	7.07
12	4.48	5.53	5.22	7.44	5.16	4.48	10.23	6.83
15	4.35	6.08	5.16	7.07	5.09	4.72	10.1	7.94
18	4.41	6.08	5.16	7.32	5.16	4.85	9.48	
21	4.29	6.27	5.34	7.44	5.47	4.97	10.1	

T_c = Torque(Newton.meter) for commercial drill
T_e = Torque(Newton.meter) for experimental drill

Table 5.5: Results of Paired Comparison Tests for Torque Data

Performance Varaible: Tss = Steady State Torque			
Speed (rpm)	Feed (mm/rev)	Test applied	Result
300	0.05	Sign Test	$M_Te > M_Tc$
600	0.05	Sign Test	$M_Te < M_Tc$
300	0.10	Sign Test	$M_Te < M_Tc$
600	0.10	Sign Test	$M_Te < M_Tc$

value of the torque is lower for the experimental drill at all cutting conditions except at the lower speed(300rpm) and feed rate(0,05mm/rev), in which case it is higher than the median value of the torque for commercial drill.

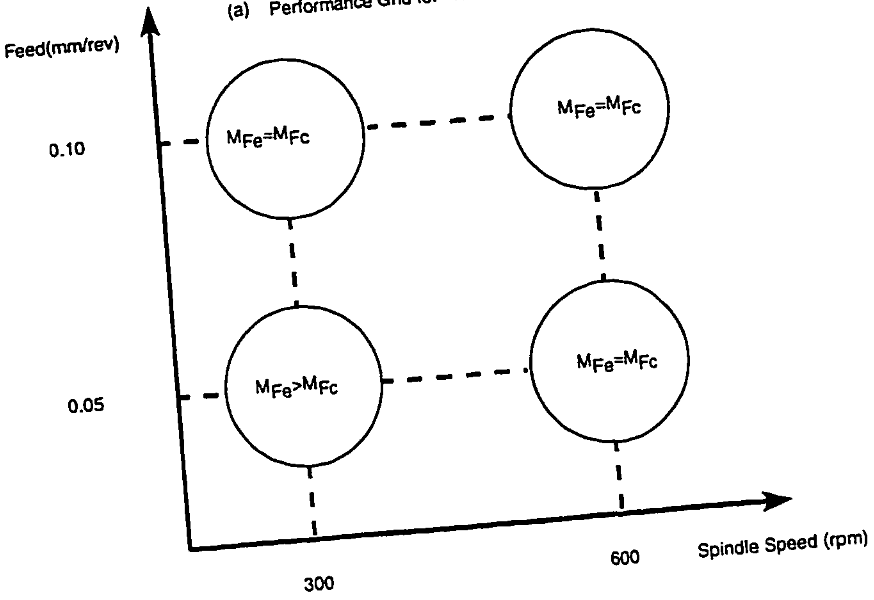
(a) Performance Grid for Thrust Force(Fss)

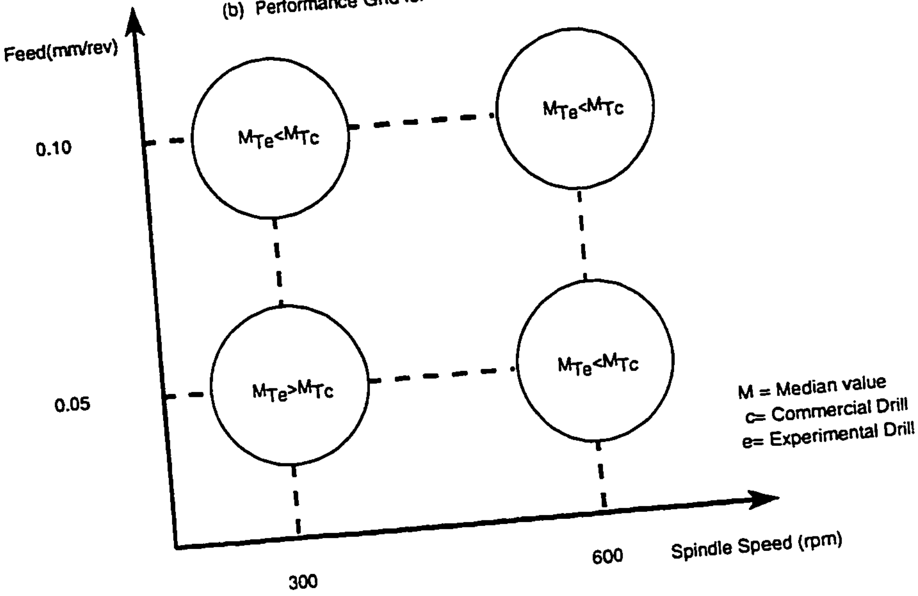
(b) Performance Grid for Drilling Torque(Tss)

Figure 5.2: Performance Grid for the (a)Thrust Force and (b)Torque as a Function of Cutting Parameters

5.3.2 The Flank Wear

The matched pair data sets values of the flank wear VB for the commercial drill and the experimental drill from hole number three to hole number twenty-one are listed in Table 5.6. This data was used for making comparative tests of the performance of the two types of drills at the four given cutting conditions following the same procedure as defined for the thrust force and torque. The results of these tests are given in Table 5.7. This table shows that for all given cutting conditions. the median values of the flank wear data sets of the experimental drills are smaller than the corresponding median values of the flank wear data sets of the commercial drills. This indicates the experimental drills have better resistance to wear. The performance grids of the two drills at the given ranges of cutting conditions with respect to flank wear are shown in Figure 5.3

Table 5.6: Flank Wear Data for Paired Comparative Tests.

Hole no	N=300rpm f=0.05mm/rev		N=300rpm f=0.10mm/rev		N=600rpm f=0.05mm/rev		N=600rpm f=0.10mm/rev	
	VB_c	VB_e	VB_c	VB_e	VB_c	VB_e	VB_c	VB_e
3	0.250	0.254	0.295	0.274	0.342	0.296	0.447	0.388
6	0.289	0.264	0.332	0.324	0.378	0.338	0.514	0.473
9	0.305	0.275	0.354	0.341	0.393	0.360	0.535	0.498
12	0.327	0.291	0.370	0.357	0.409	0.388	0.564	0.523
15	0.340	0.310	0.411	0.396	0.449	0.419	0.593	0.551
18	0.345	0.316	0.425	0.418	0.495	0.443	0.615	
21	0.364	0.326	0.439	0.426	0.508	0.462	0.646	

VB_c = Max. flank wear in mm for commercial drill
VB_e = Max. flank wear in mm for experimental drill

Table 5.7: Results of Paired Comparison Tests for Wear Data

<table>
<tr><th colspan="4">Performance Varaible: V_B = Flank Wear in mm</th></tr>
<tr><th>Speed (rpm)</th><th>Feed (mm/rev)</th><th>Test applied</th><th>Result</th></tr>
<tr><td>300</td><td>0.05</td><td>ST</td><td>$MV_{Be} < MV_{Bc}$</td></tr>
<tr><td>600</td><td>0.05</td><td>WSRT</td><td>$MV_{Be} < MV_{Bc}$</td></tr>
<tr><td>300</td><td>0.10</td><td>ST</td><td>$MV_{Be} < MV_{Bc}$</td></tr>
<tr><td>600</td><td>0.10</td><td>ST</td><td>$MV_{Be} < MV_{Bc}$</td></tr>
<tr><td colspan="4">ST = Sign Test; WSRT = Wilcoxon's Signed Rank Test</td></tr>
</table>

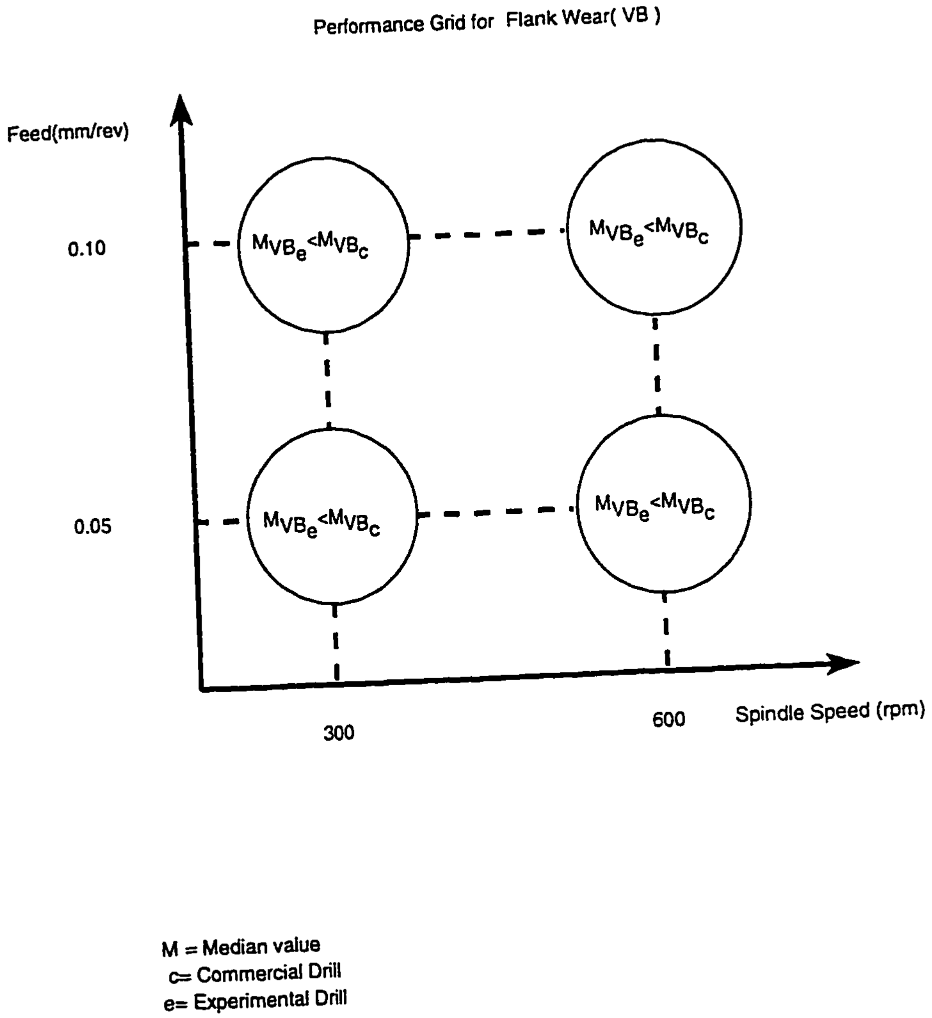

Figure 5.3: Performance Grid for the Flank Wear as a Function of Cutting Parameters

5.3.3 Drilled Hole Surface Roughness

The paired data sets of the surface roughness values obtained from Table 4.4 and Table 4.4 are tabulated in Table 5.8. The results of the matched paired testing for the surface roughness data at the given cutting conditions are listed in Table 5.9. In general and in the given ranges of cutting conditions, the median values of the drilled hole surface roughness appears to be consistantly lower for the experimental drill as compared to the commercial drill. This may be attributed to the type of TiN coating treatment applied to the experimental drill. The performance grid of the surface roughness is shown in Figure 5.4. In general the experimental drill seems to be relatively better than the commercial drill as far as the tool flank wear and the drilled hole surface roughness is concerned.

Table 5.8: Hole Surface Roughness Data for the Matched Pair Comparative Tests.

Hole no	N=300rpm f=0.05mm/rev		N=300rpm f=0.10mm/rev		N=600rpm f=0.05mm/rev		N=600rpm f=0.10mm/rev	
	R_c	R_e	R_c	R_e	R_c	R_e	R_c	R_e
1	6.05	6.23	6.52	5.66	5.02	4.3	6.53	5.64
2	6.15	4.58	6.80	5.20	5.60	3.59	6.35	5.03
3	6.37	4.35	6.66	5.63	5.18	3.83	6.29	5.30
4	6.71	4.50	7.86	5.90	5.64	4.38	6.54	5.12
5	7.51	4.60	7.50	5.64	6.61	4.293	7.09	5.73
6	7.99	5.09	8.14	6.13	7.20	4.45	7.97	5.28
7	8.71	4.89	9.96	6.49	7.31	4.60	9.07	6.02
8	9.12	5.34	9.78	6.76	8.54	4.90	9.29	5.67
9	9.79	5.31	10.45	6.58	8.34	4.77	9.66	6.43
10	9.24	5.58	10.28	7.13	8.54	5.54	10.35	7.79
11	9.61	6.12	10.58	7.58	8.16	4.94	10.02	8.47
12	9.61	6.55	11.01	7.78	8.73	5.75	10.11	7.55
13	9.92	6.35	10.77	8.30	8.55	6.15	10.00	9.91
14	10.54	6.92	12.13	8.88	9.25	6.44	10.01	10.73
15	11.22	7.35	12.13	8.57	10.14	7.42	11.36	10.03
16	11.09	7.65	11.56	9.26	9.72	7.33	10.92	
17	11.57	7.84	12.16	9.68	9.83	7.73	12.03	
18	12.33	8.52	12.86	10.22	11.59	8.27	12.32	
19	12.77	8.87	12.94	10.42	11.82	8.31	12.51	
20	12.89	8.78	13.36	10.43	12.08	8.84	13.01	
21	12.83	8.85	13.39	10.56	12.06	8.65	13.02	

R_c = Surface roughness value in μm for commercial drill
R_e = Surface roughness value in $\mu m$for experimental drill

Table 5.9: Results of Paired Comparison Tests for Roughness Data

Performance Varaible: R_a = Surface roughness (CLA μm)			
Speed (rpm)	Feed (mm/rev)	Test applied	Result
300	0.05	ST	$MR_e < MR_c$
600	0.05	ST	$MR_e < MR_c$
300	0.10	ST	$MR_e < MR_c$
600	0.10	ST	$MR_e < MR_c$
ST = Sign Test; SRT = Signed Rank Test			

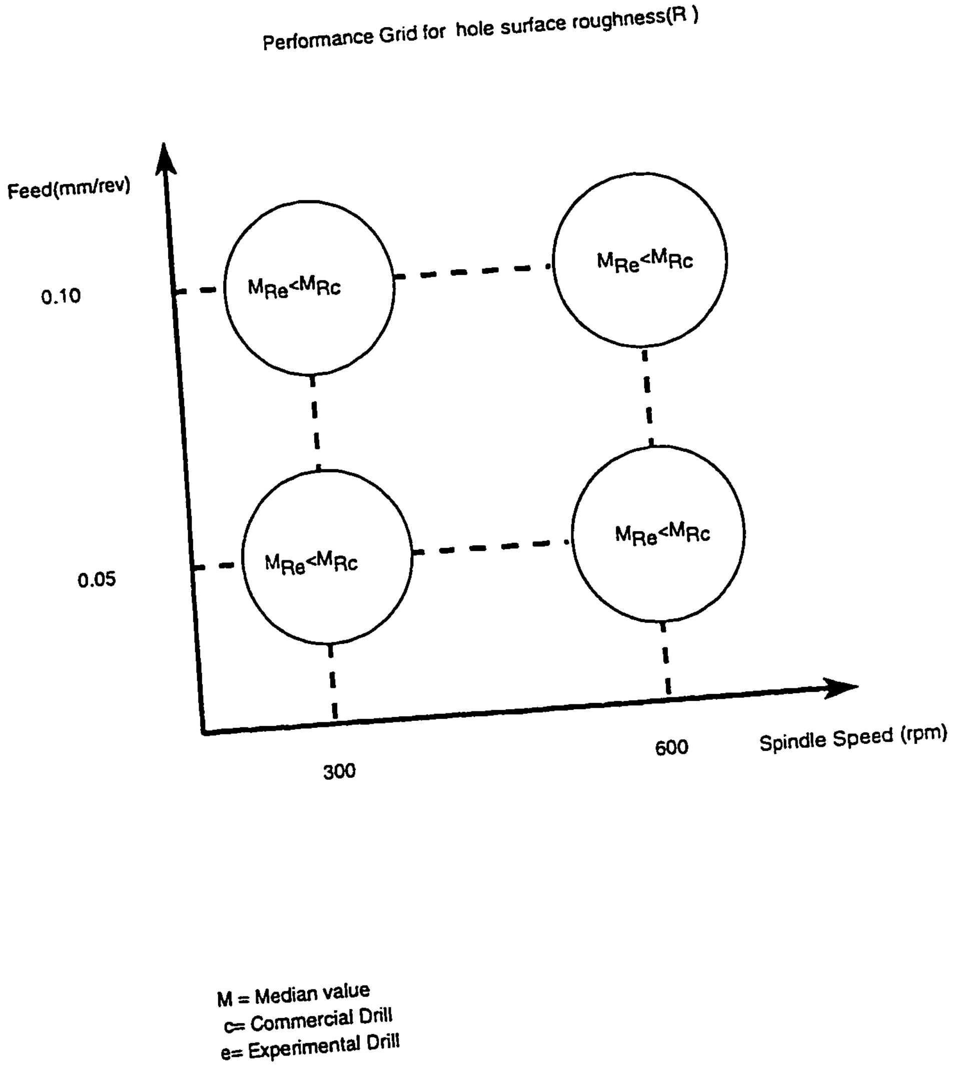

Figure 5.4: Performance Grid for the Hole Surface Roughness as a Function of Cutting Parameters

Chapter 6

CONCLUSIONS AND RECOMMENDATIONS

6.1 General Conclusions

The machining performance of a new type of Titanium Nitride (TiN) coated twist drill on which plasma nitriding was done prior to application of TiN coating to obtain an intermediate nitrided layer, was evaluated and compared to the performance of commercial TiN coated twist drills. To compare the performance, the drilling thrust force, torque, drill wear and hole surface roughness was obtained by conducting machining experiments on AISI303 stainless steel workpiece material using both types of drills. The wear patterns of the flank face and chisel edge of both types of drills were also obtained by micro-PIXE analysis. In general the experimental drill showed relatively better performance compared to the commercial drill as was observed from its higher tool life, better surface roughness, lower values of drilling torque and better adhesion of the TiN coat to the substrate material.

The detailed conclusions derived from the investigations done in this research are as follows:

- From the factorial experiments conducted to evaluate the effects of the cutting parameters on the steady state drilling thrust force and torque, it was found that the main effects of the cutting speed, feed rate and also their interaction are statistically significant at the 95% confidence interval on the thrust force as well as the torque for both experimental and commercial drills. Because of the presence of significant interaction effect for both the thrust force and torque, it is not possible to interpret the individual effects of either the speed or the feed rate.

- In general for both the experimental and the commercial drills the steady state thrust force tends to increase with the feed rate. The effect of increasing the cutting speed is to decrease the thrust force.

- Wear tests were also conducted at the given cutting conditions to evaluate the effect of drilling time on the drill flank wear. Tool life curves were plotted from the flank wear data. The values of Taylor's tool life constants 'n' and 'C' were also determined for both types of coated drills. The values of 'n' and 'C' were found to be higher for the experimental drills compared to the commercial drills. This shows that the experimental drills have a higher tool life compared to the commercial drills.

The matched paired testing method was introduced to quantitatively compare the drilling thrust force, torque, flank wear and drilled hole surface roughness data.

The following conclusions were drawn from the results of these tests:

- The median values of the thrust force, for both types of drills was found to be equal in the given ranges of cutting conditions except at the low levels of speed and feed at which, the experimental drill showed higher values than the commercial drill.
- The median values of the drilling torque for the experimental drills was found to be less than that of the commercial drills at the given range of cutting conditions except at the lowest value of speed and feed, where the experimental drill showed higher values.
- The median values of the flank wear for the experimental drills was found to be less compared to the values of the flank wear for the commercial drills at all cutting conditions.
- The median values of the surface roughness for the experimental drills were also found to be less than those for the commercial drills. The lower values of flank wear and surface roughness observed for the experimental drills are attributed to the relatively thicker TiN coating of the experimental drill compared to the commercial drills.

From the Micro PIXE results it was established that the wear on the flank face of the experimental drill takes place by abrasion. The nitriding treatment on the experimental drill prior to coating prevents the work material from adhering on this nitrided layer, while adhesion of the work material to the exposed tool surface away from the nitrided region. On the other hand, for the commercial drill wear on the flank face takes place mainly by cracking and flaking-off of the coating followed by adhesion of the work material on the exposed tool surface. This observation has been obtained by micro-PIXE analysis for the first time and hence shows its usefulness in tool wear studies. On the chisel edge of the experimental drill the boundary of the TiN coat is smooth indicating abrasive wear. Abrasive wear of TiN is possible only if it is strongly bonded to the substrate. This evidence suggests that the TiN coating on the experimental drill has a better adhesive bond to the substrate compared to the commercial drill. The chisel edge of the commercial drill had completely worn and chipped out and it was not clearly visible in the electron map. The coat on the chisel edge seems to have flaked off. The center of the chisel edge also showed evidence of MnS from the work material.

6.2 Recommendations for Future Work

The concepts developed in this study can be utilized to further investigate the effect of using a nitrided layer between the HSS substrate and the TiN coating in machining other workpiece materials not used in this study. The limited range of cutting conditions which were used in this study were based on those recommended by the manufacturer of the commercial TiN coated drills. The effect of using more severe cutting conditions on the tool life and overall drill performance can also be investigated. The results obtained from the micro-PIXE analysis of drill wear are based on the selected cutting condition of speed = 600 rpm and feed rate = 0.05 mm/rev only. The Mo distribution on the flank face of the commercial drill, and the difference in wear patterns on the chisel edges were not fully understood and hence needs further investigation. In future studies this technique can also be applied to investigate the wear behavior at different cutting conditions.

Bibliography

[1] Billau, D.J. and Heginbotham, W.B. "Some Aspects of Drill Performance and Testing". *Advances in Machine Tool Design and Research*, pages 1035–1050, 1968.

[2] Yilbas, B.S. and Sahin, A.Z. and Ahmad, Z. and AbdulAleem, B.J. "A Study of the Corrosion Properties of TiN Coated and Nitrided Ti-6Al-4V". *Corrosion Science*, 37:1627–1636, 1995.

[3] Shuaib, A.N. and Nickel, J. and Ahmed, M. "Wear Studies of Tungsten Carbide Cutting Tools using the Micro-PIXE technique". *Nuclear Instruments and Methods in physics research -B*, 103:68–72, 1995.

[4] Shaw, M.C. *Metal Cutting Principles*, page 351. Oxford Science Publications. 1st edition, 1991.

[5] Pai, A.K. and Bhattacharyya, A. and Sen, G.C. "Investigation of the Torque in Drilling Ductile Materials". *International Journal of Machine Tool Design and Research*, 4:205–221, 1965.

[6] McPhee, M.A. and Subramanian, C. and Strafford, K.N. and Wilks. T.P. and Ward, L.P. "Evaluation of Coated Twist Drills using Frequency- Domain Analysis". *Surface and Coatings Technology*, 71:215–221, 1995.

[7] Shaw, M. C. and Oxford, C.J. "On the Drilling of Metals, 2- The Torque and Thrust in Drilling". *Trans. of the American society of Mechanical Engineers*, 79:139–148, 1957.

[8] Ham, I. and Ermer, D. S. "Cutting Performance Comparison of Titanium and Tungsten Carbide Tools in Machining of Gray Iron". *Proceedings of 9th International MTDR Conference*, pages 1005–1017, 1968.

[9] Subramanian, K. and Cook, N.H. "Sensing of Drill Wear and Prediction of Drill Life". *ASME Transactions: Journal of Engineering for Industry*, 1977.

[10] Lenz, E. and Mayer, J.E.S. and Lee, D.G. "Investigation in Drilling". *Annals of CIRP*, 27:49–52, 1978.

[11] Osman, M.O.M. and Xistris, G.D. and Chahil, G.S. "The Measurement and Stochastic Modelling of Torque and Thrust in Twist Drilling". *International of Production Research*, 17:359–376, 1979. IMP.

[12] Thangaraj, A. and Wright, P.K. "Computer Assisted Prediction of Drill-Failure Using In-Process Measurements of Thrust Force". *ASME Transactions: Journal of Engineering for Industry*, 110:192–199, 1988.

[13] Jalali, S.A. and Kolarik, W.J. "Tool Life and Machinability Models for Drilling Steels". *International Journal of Machine Tools and Manufacture*. 31-3:273–282, 1991.

[14] Rubenstein, C. "The Torque and Thrust Force in Twist Drilling-I". *International Journal of Machine Tools and Manufacture*, 31:491-504, 1991.

[15] Agapiou, J.S. "Design Characteristics of New Types of Drill and Evaluation of Their Performance Drilling Cast Iron-I". *International Journal of Machine Tools and Manufacture*, 33:343–365, 1993.

[16] Lin, S.C. and Ting, C.J. "Drill Wear Monitoring Using Neural Networks". *International Journal of Machine Tools and Manufacture*, 36:465–475, 1995.

[17] Watson, A.R. "Drilling Model for Cutting Lip and Chisel Edge and Comparison of Experimental and Predicted Results-IV". *International Journal of Machine Tool Design and Research*, 25:393–404, 1985.

[18] Sadat, A.B. "Surface Characteristics of Machined Inconel-718 Nickel-Base Superalloy using Natural and Controlled Contact Length Tools". *International Journal of Machine Tools and Manufacture*, 27:333–342, 1987.

[19] Venkatesh, V.C. *Experimental Techniques in Metal Cutting.* Prentice Hall of India, 1987.

[20] Subramanian, C. and Strafford, K.N. and Wilks, T.P. and Ward, L.P. and McPhee, M.A. "Performance Evaluation of TiN-Coated Twist Drills Using Force Measurement and Microscopy". *Surface and Coatings technology*, 62:641–648, 1993.

[21] Henderer, W.E. "Performance of Titanium Nitride Coated High Speed Steel Drills". *11th NAMRC*, pages 337–341, 1983.

[22] Dearnley, P.A. and Trent, E.M. "Wear Mechanisms of Coated Carbide Tools". *Metals Technology*, 9:60–74, 1982.

[23] Konig, G. and Kauven, R. and Droese, A. "Improved HSS Tool Performance with Mechanically Resistant Coatings". *CIRP Annals*, 35-1:31–36, 1986.

[24] Randhawa, H. "TiN Coated High Speed Steel Cutting Tools". *Journal of Vaccum Science Technology*, 6:2755–2758, 1986.

[25] Munz, W.D. "Titanium Aluminum Nitride Films: A New Alternative to TiN Coatings". *Journal of Vaccum Science Technology*, 6:2717–2725, 1986.

[26] Konig, W. and Fritsch, R. and Kammermeier, D. "Physically Vapor Deposited Coatings on Tools: Performance and wear Phenomena". *Surface and Coatings Technology*, 49:316–324, 1991.

[27] Molarious, J.M. and Korhonen, A.S. and Kankaanpaa, H. and Sulonen, M.S. "Turning Performance of Reactively Ion Plated Ti-N Coatings". *Journal of Vaccum Science Technology*, 6:2686–2690, 1986.

[28] Soliman, F. A. and Abu-Zeid, O.A. "On the Improvement of The Performance of High Speed Steel Turning Tools By TiN Coatings". *Wear*, 119:199–204, 1987.

[29] Wallen, P. and Hogmark, S. "Influence of TiN Coating on Wear of High Speed Steel at Elevated Temperature". *Wear*, 130:123–135, 1989.

[30] Ahmed, M. and Nickel, J. and Hallak, A.B. and Abdel-Aal, R.E. and Coban, A. Al-Juwair, H.A. "The KFUPM Scanning Nuclear Microprobe Facility". *Nuclear Instruments and Methods-B*, 82:584–588, 1993.

[31] Maxwell, J.A. *Thick/Thin Target Interactive PIXE Routine Users Guide.* University of Guelph Physics department, 1993.

[32] Devor, R.E. and Chang, T. and Sutherland, J.W. *Statistical Quality Design and Control*, pages 585–605. Macmillan, 1st edition, 1992.

[33] Box J.E.P. and Hunter W.G and Hunter J.S. *Statistics for Experimenters-An Introduction to Design Data Analysis and Model Building*, pages 306–324. John Wiley and Sons, 1978.

[34] Statistical Graphics Corporation . *Statgraphics Plus Version-1: User Manual*. pages 9–18. Manugistics Inc., 1st edition, 1994.

[35] Boothroyd, G. *Fundamentals of Metal Machining and Machine Tools*. pages 110–111. McGraw Hill International Book Company, 1st edition, 1975.

[36] Tipnis, V.A. and Christopher, J.D. "Machinability Testing for Industry". *Proceedings of International Conference on Machinability Testing and Utilization of Machinability Data*, pages 3–35, 1979.

[37] Schey, J.A. *Introduction to Manufacturing Processes*, page 464. McGraw Hill International Book Company, 2nd edition, 1987.

[38] . *Metals Handbook*, volume 1, pages 842–843. American Society of Metals. 10th edition, 1990.

[39] Leyendecker, T. and Lemmer, O. and Esser, S. "The Development of the PVD coating TiAlN as a Commercial Coating for Cutting Tools". *Surface and Coatings Technology*, 48:175–178, 1991.

[40] Lapin, L.L. *Probability and Statistics for Modern Engineering*. page 408. PWS Publishers., 1983.

Vita

- SYED MOHTASHIM NIZAM
- Born in India.
- Permanent Address :
  H.No. 2-2-1108/2 , Tilaknagar,
  Hyderabad 500044, A. P., INDIA, Ph.0091-46-4052925.
- Received Bachelor of Engineering (**B.E.**) degree in Mechanical Engineering from Osmania University, Hyderabad, India 1990.
- Received Master of Bussiness Administration (**M.B.A.**) degree from Osmania University, Hyderabad, India 1992.
- Received Master of Science (**M.S.**) degree in Mechanical Engineering from King Fahd University of Petroleum and Minerals, Dhahran, Saudi Arabia in 1996.